

# **The Effect of Meteorological Conditions and Atmospheric Composition in the Occurrence and Development of New Particle Formation (NPF) Events in Europe**

**Dimitrios Bousiotis<sup>1</sup>, James Brean<sup>1</sup>, Francis Pope<sup>1</sup>, Manuel Dall'Osto<sup>2</sup>  
Xavier Querol<sup>3</sup>, Andres Alastuey<sup>3</sup>, Noemi Perez<sup>3</sup>, Tuukka Petäjä<sup>4</sup>  
Andreas Massling<sup>5</sup>, Jacob Klenø Nøjgaard<sup>5</sup>, Claus Nørdestrom<sup>5</sup>  
Giorgos Kouvarakis<sup>6</sup>, Stergios Vratolis<sup>7</sup>, Konstantinos Eleftheriadis<sup>7</sup>  
Jarkko V. Niemi<sup>8</sup>, Harri Portin<sup>8</sup>, Alfred Wiedensohler<sup>9</sup>, Kay Weinhold<sup>9</sup>, Maik  
Merkel<sup>9</sup>, Thomas Tuch<sup>9</sup> and Roy M. Harrison<sup>1a\*</sup>**

**<sup>1</sup>Division of Environmental Health and Risk Management  
School of Geography, Earth and Environmental Sciences  
University of Birmingham, Edgbaston, Birmingham B15 2TT, United Kingdom**

**<sup>2</sup>Institute of Marine Sciences, Passeig Marítim de la Barceloneta, 37-49 E-08003  
Barcelona, Spain**

**<sup>3</sup>Institute of Environmental Assessment and Water Research (IDAEA - CSIC)  
08034, Barcelona, Spain**

**<sup>4</sup>Institute for Atmospheric and Earth System Research (INAR) / Physics, Faculty of Science  
University of Helsinki, Finland**

**<sup>5</sup>Department for Environmental Science, Aarhus University, DK-400, Roskilde, Denmark**

**<sup>6</sup>Environmental Chemical Processes Laboratory (ECPL), Department of Chemistry,  
University of Crete, 70013, Heraklion, Greece**

**<sup>7</sup>Environmental Radioactivity Laboratory, Institute of Nuclear and Radiological Science &  
Technology, Energy & Safety, NCSR Demokritos, Athens, Greece**

**<sup>8</sup>Helsinki Region Environmental Services Authority (HSY),  
FI-00066 HSY, Helsinki, Finland**

**<sup>9</sup>Leibniz Institute for Tropospheric Research (TROPOS),  
Permoserstr. 15, 04318 Leipzig, Germany**

39 <sup>a</sup>Also at: Department of Environmental Sciences / Center of Excellence in Environmental  
40 Studies, King Abdulaziz University, PO Box 80203, Jeddah, 21589, Saudi Arabia  
41

## 42 ABSTRACT

43 Although new particle formation (NPF) events have been studied extensively for some decades, the  
44 mechanisms that drive their occurrence and development are yet to be fully elucidated. Laboratory  
45 studies have done much to elucidate the molecular processes involved in nucleation, but this  
46 knowledge has yet to be conclusively linked to NPF events in the atmosphere. There is great  
47 difficulty in successful application of the results from laboratory studies to real atmospheric  
48 conditions, due to the diversity of atmospheric conditions and observations found, as NPF events  
49 occur almost everywhere in the world without always following a clearly defined trend of  
50 frequency, seasonality, atmospheric conditions or event development.

51 The present study seeks common features in nucleation events by applying a binned linear  
52 regression over an extensive dataset from 16 sites of various types (combined dataset of 85 years  
53 from rural and urban backgrounds as well as roadside sites) in Europe. At most sites, a clear  
54 positive relation is found between the solar radiation intensity (up to  $R^2 = 0.98$ ), temperature (up to  
55  $R^2 = 0.98$ ) and atmospheric pressure (up to  $R^2 = 0.97$ ) with the [probabilityfrequency](#) of NPF events,  
56 while relative humidity (RH) presents a negative relation (up to  $R^2 = 0.95$ ) with NPF event  
57 [probabilityfrequency, though exceptions were found among the sites for all the variables studied.](#)

58 Wind speed presents a less consistent relationship which appears to be heavily affected by local  
59 conditions. While some meteorological variables (such as the solar radiation intensity and RH)  
60 appear to have a crucial effect on the occurrence and characteristics of NPF events, especially at  
61 rural sites, it appears that their role becomes less marked when at higher average values.

62

63 The analysis of chemical composition data presents interesting results. Concentrations of almost all  
64 chemical compounds studied (apart from O<sub>3</sub>) and the Condensation Sink (CS) have a negative  
65 relationship with NPF event [probabilityfrequency](#), though areas with higher average concentrations  
66 of SO<sub>2</sub> had higher NPF event [probabilityfrequency](#). Particulate Organic Carbon (OC), Volatile  
67 Organic Compounds (VOCs) and particulate phase sulphate consistently had a positive relation with  
68 the growth rate of the newly formed particles. As with some meteorological variables, it appears  
69 that at increased concentrations of pollutants or the CS, their influence upon NPF  
70 [probabilityfrequency](#) is reduced.

71

## 72 1. INTRODUCTION

73 New Particle Formation (NPF) events are an important source of particles in the atmosphere  
74 (Merikanto et al., 2009; Spracklen et al., 2010). ~~These which~~ are known to have adverse effects on  
75 human health (Schwartz et al., 1996; Politis et al., 2008; Kim, et al., 2015), as well as affecting the  
76 optical and physical properties of the atmosphere (Makkonen et al., 2012; Seinfeld and Pandis,  
77 2012). While ~~they~~ NPF events occur almost everywhere in the world (Dall'Osto et al., 2018;  
78 Kulmala et al., 2017; O'Dowd et al., 2002; Wiedensohler et al., 2019; Chu et al., 2019; Kerminen et  
79 al., 2018), with some exceptions ~~mentioned in the literature~~ reported in forest (Lee et al., 2016; Pillai  
80 et al., 2013; Rizzo et al., 2010) or high-elevation sites (Bae et al., 2010; Hallar et al., 2016), great  
81 diversity is found in the atmospheric conditions within which they take place. ~~The M~~ many studies  
82 ~~have been done in~~ conducted have included many ~~a large number of~~ different types of locations  
83 (urban, traffic, regional background), around the world and differences were found in both the  
84 seasonality and intensity of NPF events. ~~To an extent~~ This variability is due may be related to the  
85 mix of conditions that are specific to each location, which ~~blurs~~ obscures the general understanding  
86 of the conditions that are favourable for the occurrence of NPF events (Berland et al., 2017;  
87 Bousiotis et al., 2020). For example, solar radiation is considered as one of the most important  
88 factors in the occurrence of NPF events (Kulmala and Kerminen, 2008; Kürten et al., 2016; Pikridas  
89 et al., 2015; Salma et al., 2011), as it ~~is needed for~~ drives the photochemical reactions ~~that~~ leading to  
90 the formation of sulphuric acid (Petäjä et al., 2009; Cheung et al., 2013). ~~which~~ Sulphuric acid is  
91 ~~considered as~~ frequently the main component of the formation and growth of the initial clusters (Iida

et al., 2008; Stolzenburg et al., 2020; Weber et al., 1995). Nevertheless, in many cases NPF events ~~did do~~ not occur in the seasons with the highest insolation (Park et al., 2015; Vratolis et al., 2019). Similarly, uncertainty exists over the effect of temperature (Yli-Juuti et al., 2020; Stolzenburg et al., 2018). Higher temperatures are considered favourable for the growth of the newly formed particles as increased concentrations of both Biogenic Volatile Organic Compounds (BVOCs) and Anthropogenic Volatile Organic Compounds (AVOCs) (Yamada, 2013; Paasonen et al., 2013) and their oxidation products (Ehn et al., 2014) ~~are associated to the~~support growth of the particles. ~~Still, On the other hand, t~~The negative effect of increased~~ed~~ temperatures ~~in increasing the energy upon the stability of barriers the molecular~~ clusters ~~have to overcome to become stable and grow in size though~~ should not be overlooked (Kürten et al., 2018; Zhang et al., 2012). ~~This~~The former factor appears ~~frequently to be true~~be dominant in most cases, as higher growth rates are found in most cases in the local summer (Nieminen et al., 2018), although the actual importance of those VOCs in the occurrence of NPF events is still not fully elucidated, with oxidation mechanisms still under intense research (Tröstl et al., 2016; Wang et al., 2020). The effect of other meteorological variables is even more complex, with studies presenting mixed results on the effect of the wind speed and atmospheric pressure. Extreme values of those variables may be favourable for the occurrence of NPF events, as they are associated with increased mixing in the atmosphere, but at the same time suppress nucleation due to increased dilution of precursors (Brines et al., 2015; Rimnácová et al., 2011; Shen et al., 2018; Siakavaras et al., 2016), or favour ~~them~~it due to a reduced condensation sink (CS).

112

113 The effect of atmospheric composition on NPF events is also a puzzle of mixed results. While the  
114 negative effect of the increased CS on the occurrence of the events is widely accepted (Kalkavouras  
115 et al., 2017 ; Kerminen et al., 2004; Wehner et al., 2007), cases are found when NPF events occur  
116 on days with higher CS compared to average conditions (Größ et al., 2018; Kulmala et al., 2005).  
117 Sulphur dioxide (SO<sub>2</sub>), which is one of the most important contributors to many NPF pathways, in  
118 most studies was found ~~in~~at lower concentrations on NPF event days compared to average  
119 conditions (Alam et al., 2003; Bousiotis et al., 2019), although there are studies that have reported  
120 the opposite (Woo et al., 2001; Charron et al., 2008). Additionally, in a combined study of NPF  
121 events in China, events were found to be more probable under sulphur-rich conditions rather than  
122 sulphur-poor (Jayaratne et al., 2017). Similar is the case with the BVOCs and AVOCs, which  
123 present great variability depending the area studied (Dai et al., 2017), and their contribution in the  
124 growth of the particles is not fully understood yet. Until recently, it was considered unlikely for  
125 NPF events, as they are considered in the present study (deriving from secondary formation not  
126 associated with traffic related processes such as dilution of the engine exhaust), to occur within the  
127 complex urban environment due to the increased presence of compounds, mainly associated with  
128 combustion processes, which would suppress the survival of the newly formed particles within this  
129 type of environment (Kulmala et al., 2017). Despite this, NPF events were found to occur within  
130 even the most polluted areas and sometimes with high formation and growth rates (Bousiotis et al.,  
131 2019; Yao et al., 2018).

132 It is evident that while a general knowledge of the role of the meteorological and atmospheric  
133 variables has been achieved, there is great uncertainty over the extent and variability of their effect  
134 (and for some of them even their direction of an actual effect) in the mechanisms of NPF in real  
135 atmospheric conditions, especially in the more complex urban environment (Harrison, 2017). The  
136 present study, using an extensive dataset from 16 sites in six European countries, attempts to  
137 elucidate the effect of several meteorological and atmospheric variables not only in general, but also  
138 depending on the geographical region or type of environment. While studies with multiple sites  
139 have been reported in the past (Dall'Osto et al., 2018; Kulmala et al., 2005; Rivas et al., 2020), to  
140 the authors' knowledge this is the first study that focuses directly on the effect of these variables  
141 upon the probability frequency of NPF events as well as the formation and growth rates of newly  
142 formed particles in real atmospheric conditions.

143

## 144 2. DATA AND METHODS

### 145 2.1 Site Description and Data Availability

146 The present study uses a total of more than 85 years of hourly data from 16 sites from six countries  
147 of Europe of various land usage and climates. It was considered very important that at least a rural  
148 and an urban site would be available from each country to study the differences between the  
149 different land usage on NPF events throughout Europe. The sites were chosen to cover the greatest  
150 possible extent of the European continent, with sites from both northern, central and southern  
151 Europe, as well as from western and eastern. The sites are located in the UK (London and Harwell),



152 Denmark (Copenhagen greater area), Germany (Leipzig greater area), Finland (Helsinki and  
153 Hyytiälä), Spain (Barcelona and Montseny – a site in a mountainous area) and Greece (Athens and  
154 Finokalia). Unfortunately, not all sites had available data for all the variables studied, which to an  
155 extent may bias some of the results. An extended analysis of the typical and NPF event conditions,  
156 seasonal variations and trends at these sites for the same period is found in other studies (Bousiotis  
157 et al., 2019; 2020). A list of the available data and a brief description for each site is found in Table  
158 1 (for the ease of reading the sites are named by the country of the site followed by the last two  
159 letters which refer to the type of site, being RU for rural/regional background, UB for urban  
160 background and RO for roadside site), while a map of the sites is found in Figure 1. For all the sites,  
161 the data used in the present study are of either 1-hour resolution or less. Data with coarser  
162 resolutions were omitted for reliability.  
163 Most of the data used in this analysis were also published in previous studies. The data from the UK  
164 were published in Bousiotis et al., (2019; 2020), while parts of it were also published in Beddows et  
165 al., (2015; 2019). The data for the German sites and parts of the data from UK, Denmark and  
166 Finland were also published in von Bismarck et al., (2013; 2014; 2015). Parts of the measurements  
167 for the Spanish sites were used in Carnerero et al., (2019) and Brines et al., (2015). The data for the  
168 Greek rural background site were published in Kalivitis et al., (2019). Finally, the data for the Greek  
169 urban background site were extracted from the European database (EBAS – ebas.nilu.no) and to the  
170 authors' knowledge has not been used in previous studies. Additional data for some of the sites  
171 were provided from their respective operators and were also not used in the past.

172

## 173 2.2 Methods

### 174 2.2.1 NPF events selection

175 NPF events were selected using the method proposed by Dal Maso et al (2005). An NPF event is  
176 identified by the appearance of a new mode or particles in the nucleation mode (smaller than 20 nm  
177 in diameter), which prevails for some hours and shows signs of growth. The events can then be  
178 classified into classes I and II according to the level of certainty, while class I events can be further  
179 classified to Ia and Ib. Events having both a clear formation of a new mode of particles in the  
180 smallest size bins available (thus excluding possible advected events) as well as a distinct and  
181 persistent growth of the new mode of particles for at least 3 hours were classified as Ia, while Ib  
182 consists of rather clear events that fail though by at least one of the criteria set. Additionally, for the  
183 roadside sites, a formation of particles in the nucleation mode accompanied by a significant increase  
184 of the concentrations of pollutants was not considered as an NPF event, as it may be associated with  
185 mechanisms other than the secondary formation. In the present study, only the events of class Ia  
186 were considered with the additional criterion of at least  $1 \text{ nm h}^{-1}$  growth for at least 3 hours. [As the](#)  
187 [available SMPS datasets for the sites in the U.K. are for particles of diameter greater than 16 nm,](#)  
188 [additional criteria were set to ensure the correct extraction of NPF events, including the variations](#)  
189 [of the particle number concentrations from a Condensation Particle Counter \(CPC – measuring](#)  
190 [particles with diameter from 7nm\), as well as of the concentrations of gaseous pollutants and](#)  
191 [aerosol constituents \(please refer to the Methods section in Bousiotis et al., 2019\).](#)

## 2.2.2 Calculation of condensation sink, growth rate, formation rate, and NPF event

probability frequency

The condensation sink (CS) is calculated according to the method proposed by Kulmala et al., (2001) as:

$$CS = 4\pi D_{vap} \sum \beta_M r N \quad (1)$$

where  $r$  and  $N$  is the radius and number concentration of the particles respectively and  $D_{vap}$  is the diffusion coefficient calculated as (Poling et al., 2001):

$$D_{vap} = 0.00143 \cdot T^{1.75} \frac{\sqrt{M_{air}^{-1} + M_{vap}^{-1}}}{P \left( D_{x,air}^{\frac{1}{3}} + D_{x,vap}^{\frac{1}{3}} \right)^2} \quad (2)$$

for  $T = 293$  K and  $P = 1013.25$  mbar.  $M$  and  $D_x$  are the molar mass and diffusion volume for air and sulphuric acid.  $\beta_M$  is the Fuchs correction factor calculated as (Fuchs and Sutugin, 1971):

$$\beta_M = \frac{1 + K_n}{1 + \left( \frac{4}{3a} + 0.377 \right) K_n + \frac{4}{3a} K_n^2} \quad (3)$$

209 where  $K_n$  is the Knudsen number, calculated as  $K_n = 2\lambda_m/d_p$  where  $\lambda_m$  is the mean free path of the  
210 gas. It should be noted that due to the lack of sufficient chemical composition data for a number of  
211 sites, the CS calculated is not corrected for hygroscopic growth. As a result, the values for CS and  
212 the results associated to it presented in this work, may be biased between the sites studied due to the  
213 great differences in the conditions between them.

214  
215 Growth rate (GR) is calculated as (Kulmala et al., 2012):

216  
217 
$$GR = \frac{D_{P_2} - D_{P_1}}{t_2 - t_1} \quad (4)$$

218  
219 for the size range between the minimum available particle diameter up to 30 nm (50 nm for the UK  
220 sites due to the higher minimum particle size available). The time window used for the calculation  
221 of the growth rate was from the start of the event until a) growth stopped, b) GMD reached the  
222 upper limit set or c) the day ended.

223  
224 The formation rate  $J$  was calculated using the method proposed by (Kulmala et al., 2012) as:

225  
226 
$$J_{dp} = \frac{dN_{dp}}{dt} + \text{Coag}S_{dp} \times N_{dp} + \frac{GR}{\Delta d_p} \times N_{dp} + S_{losses} \quad (5)$$

228 where  $\text{CoagS}_{dp}$  is the coagulation rate of particles of diameter  $d_p$ , calculated as (Kerminen et al.,  
 229 2001):

230

$$231 \quad \text{CoagS}_{dp} = \int K(d_p, d'_p) n(d'_p) dd'_p \cong \sum_{d'_p=d_p}^{d'_p=\max} K(d_p, d'_p) N_{dp} \quad (6)$$

232

233  $K(d_p, d'_p)$  is the coagulation coefficient of particles with diameters  $d_p$  and  $d'_p$ , while  $S_{\text{losses}}$  accounts  
 234 for additional loss terms (i.e. chamber wall losses), which are not applicable in the present study.  
 235 For the present study, the formation rate of particles of diameter of 10 nm was calculated for  
 236 uniformity (16 nm for the UK sites), though most sites had data for particle sizes below 10 nm.

237

238 The NPF ~~probability frequency, used instead of NPF frequency when modelled results are presented,~~  
 239 was calculated by the number of NPF event days divided by the number of days with available data  
 240 in the given group (full dataset or temporal, variable ranges etc.). The results presented in this study  
 241 were normalised according to the data availability, as:

242

$$243 \quad NPF_{\text{probability frequency}} = \frac{N_{\text{NPF event days for group of days } X}}{N_{\text{days with available data for group of days } X}} \quad (76)$$

244 Finally, the p-values reported in the analysis derive from the ANOVA one-way test. As the  
 245 normality of the variables is required for such an analysis, the Shapiro-Wilk test was used to assess

the normality and the vast majority of the variables were found to have  $p > 0.05$  and thus were considered as normal. This is probably due to the removal of the extreme values (as mentioned in section 2.2.3, for the calculations 90% of each dataset was kept removing the extremely high and/or low values and the possible outliers included in them). While this was not done to promote the normality of the populations but to reduce the bias from extreme values, it indirectly assisted in making the distributions normal. For the few remaining (e.g. the growth rates associated with SO<sub>2</sub> concentrations for UKRO) for which normality was not present, the square root of the values of the variable were considered to achieve normality and proceed to the ANOVA test.

### 2.2.3 Calculation of the gradient and intercept for the variables used

Due to the large datasets available and the great spread of the values, a direct comparison between a given variable and any of the characteristics associated with NPF events (NPF ~~probability~~frequency, growth rate and formation rate) always provided results with low statistical significance. As a result, an alternative method which can provide a reliable result without the dispersion of the large datasets was used in the present study, to investigate the relationships between the variables which are considered to be associated with the NPF events. For this, a timeframe which is more directly associated with the NPF events typically observed in the mid-latitudes was chosen. For NPF ~~probability~~frequency and GR the timeframe between 05:00 to 17:00 Local Time (LT) was chosen, which is considered the time when the vast majority of NPF events take place and further develop with the growth of the particles. For the formation rate a smaller

266 timeframe was chosen, 09:00 to 15:00 LT which is  $\pm 3$  hours from the time of the maximum  
267 formation rate found for almost all sites (12:00 LT). This was done to exclude as far as possible the  
268 effect of the morning rush at the roadside sites, as well as only to include the time window when the  
269 formation rate is mostly relevant to NPF events (negative values that are more probable outside this  
270 timeframe and are not associated with the formation of the particles would bias the results).

271  
272 For the CS the timeframe 05:00 to 10:00 LT was chosen. This was done to avoid including the  
273 direct effect of the NPF events (the contribution of newly formed particles to CS), as well as to  
274 provide results for the conditions which either promote or suppress the characteristics studied,  
275 which specifically for the CS are more important before the start of the events. The extreme values  
276 (very high or very low) which bias the results only carrying a very small piece (forming bins of very  
277 small size) of information were then removed, though 90% of the available data was used for all the  
278 variables. The ~~data left~~remaining data was separated into smaller bins and a minimum of 10 bins  
279 was required for each variable (for example if the difference between the minimum and the  
280 maximum relative humidity (RH) is 70%, then 14 bins each with a range of 5% were formed). The  
281 variables of interest were then averaged for each bin and plotted, and a linear relation was  
282 considered for each one of them. While it is evident that not all relationships are linear, the specific  
283 type was chosen in the present analysis for all the variables studied. This was done because the aim  
284 was to elucidate the general positive or negative effect of the variables studied. Furthermore, the  
285 effect of many variables appears to vary between sites with great differences (either geographical or

286 type of land use) and the choice of a single method to describe these relationships ensures the  
287 uniformity of the results, as it appears to better describe them in most cases.  
288

289 The gradient of these linear relations ( $a_N$ ,  $a_G$  and  $a_J$  for NPF probabilityfrequency, growth rate and  
290 formation rate  $J_{10}$  accordingly) found in this analysis should be used with great caution as apart  
291 from the atmospheric conditions (local and meteorological as well as atmospheric composition) it is  
292 also affected by the variable in question (e.g. a greater NPF probabilityfrequency will provide a  
293 greater gradient), resulting in giving the same trend for all the atmospheric variables tested; the sites  
294 with the higher values of these variables (NPF probabilityfrequency and formation rate) always had  
295 greater gradient values and vice versa. In order to remove the effect of the variable in question  
296 (NPF probabilityfrequency or formation rate – growth rate will provide an unreliable result as it is  
297 calculated in a different range for each site due to the lower available size of particles), the gradients  
298 were normalised by dividing them by their respective variable (e.g. divide the gradient of the NPF  
299 probabilityfrequency with the NPF frequency), providing with a new normalised slope ( $a_N^*$  for NPF  
300 probabilityfrequency or  $a_J^*$  for the formation rate) that will have no significance other than its  
301 absolute value, which can be used for direct comparisons:

302 
$$a_N^* = \frac{a_N}{\text{NPF \%}}$$

303 Where  $a_N$  is the gradient of the relation between the given variable and NPF frequency (NPF %)

304



$$a_J^* = \frac{a_J}{J_{10}}$$

Where  $a_J$  is the gradient of the relation between the given variable and the formation rate of 10 nm particles  $J_{10}$  ( $J_{16}$  for the UK sites).

### 3. RESULTS

In this study NPF events are generally observed as particles grow from a smaller size (typically 3-16 nm depending on the size detection limit of instruments used) to 30 nm or larger. They therefore reflect the result both of nucleation, which creates new particles of 1-2 nm (not detected with the instruments used in this study), and growth to larger sizes. In analysing NPF events, we therefore consider three diagnostic features:

- the probabilityfrequency of events occurring (i.e. days with an event divided by total days with relevant data, depending on the variable and range studied). As only class Ia events were only considered, it is expected that the frequency of the events calculated should be lower than the expected one if all types of events were included. This could result in values up to one third of those anticipated if all types of events were considered. For the extent of this variation please refer to Bousiotis et al., (2019; 2020) in which there is an extended analysis of the NPF events for each site, including the special cases of NPF events that do not comply for the criteria set for class Ia.

- the rate of particle formation at a given size ( $J_{10}$  in this case), which was found to have unclear seasonal trends among the sites and was higher for urban sites compared to rural in most cases (Bousiotis, 2019; 2020)
- the growth rate of particles from the lower measurement limit to 30 nm (or 50 nm for the UK sites), which was found to be greater during summer months for most of the sites, also studied in the aforementioned works.-

From the analysis of the extended dataset a total of 1952 NPF events were extracted and studied.

The NPF frequency, growth and formation rate for each site is found in Table 2. The seasonal variation of NPF events is found in Figure S14.

### 3.1 Meteorological Conditions

The gradients, coefficients of determination ( $R^2$  – the relationships found are characterised as weak for  $R^2 < 0.50$ , strong for  $0.50 < R^2 < 0.75$  and very strong for  $R^2 > 0.75$ ) and the p-values ~~(deriving from one-way ANOVA test)~~ from the analysis of the meteorological variables, as well as the average conditions of these variables are found in Table 3. The results for each site and variable are found in figures S1 – S5.

#### 3.1.1 Solar radiation intensity

As mentioned earlier, solar radiation intensity is considered to be one of the most important variables in NPF occurrence, as it contributes to the production of  $H_2SO_4$  which is a main

343 component of the initial clusters and participates in the early growth of the newly formed particles.  
344 Hidy et al. (1994) reported up to six times higher SO<sub>2</sub> oxidation rates into H<sub>2</sub>SO<sub>4</sub> in typical summer  
345 conditions compared to winter. For almost all sites this relation is confirmed with very strong  
346 correlations ( $R^2 > 0.75$ ) between the intensity of solar radiation and the [probabilityfrequency](#) for  
347 NPF events to occur. The relationship between the solar radiation and NPF [probabilityfrequency](#)  
348 was positive at all sites and only three sites (FINUB, SPARU and GREUB) presented weak  
349 correlations ( $R^2 < 0.40$ ). Weaker correlations were found for the southern European sites, which  
350 might be associated with the higher averages for solar radiation intensity, or the interference of  
351 other processes (such as coinciding with increased CS by recirculation of air masses (Carnerero et  
352 al., 2019)), possibly making it less of an important factor for these areas.

353  
354 The relationship of solar radiation with the growth rate was weaker in all cases and did not present a  
355 clear trend. Only some rural background sites (GERRU, FINRU and GRERU)- presented a strong  
356 correlation ( $R^2 > 0.50$ ). The relationship found in most cases was positive apart from two roadside  
357 sites (GERRO and UKRO) and two urban background sites (GREUB and UKUB), though due to  
358 the low  $R^2 (< 0.10)$  these results cannot be considered with confidence. It seems though that the  
359 solar radiation intensity is probably a more important factor at background sites rather than at  
360 roadside sites, where possibly local conditions (such as local emissions) are more important (Olin et  
361 al, 2020). Finally, the formation rate has a positive relationship with the solar radiation intensity,  
362 with relatively strong correlations in most areas ( $R^2 > 0.50$ ). The correlations were stronger at the

363 rural background sites compared to the roadside sites, which further underlines the increased  
364 importance of this factor at this type of site. A negative relationship between the solar radiation  
365 intensity and the formation rate was found at the GRERU site but the  $R^2$  is very low ( $R^2 = 0.05$ ).

366  
367 Plotting the normalised gradients for NPF event ~~probability~~frequency  $a_N^*$  with the average solar  
368 radiation intensity at each site (Figure 2) a negative relationship is found ( $R^2 = 0.62$ ), with the  
369 southern areas (those with higher average solar intensity) having smaller  $a_N^*$  compared to those in  
370 higher latitudes (and thus with a lower average solar radiation). This may indicate that while solar  
371 radiation is a deciding factor in the occurrence of an NPF event, when in greater intensity its role  
372 becomes relatively less important, a finding that was also implied by Wonaschütz et al. (2015).  
373 Additionally, the  $a_r^*$  was found to be higher at all rural sites compared to their respective roadside  
374 sites (and urban background sites for all but the Greek and German ones), making it a more  
375 important factor at this type of site (Figure 3).

376

### 377 3.1.2 Relative humidity

378 Relative humidity is considered to have a negative effect on the occurrence of NPF events (Jeong et  
379 al., 2010; Hamed et al., 2011; Park et al., 2015; Dada et al., 2017; Li et al., 2019). While water in  
380 the atmosphere is one of the main compounds needed for the formation of the initial clusters either  
381 on the binary or ternary nucleation theory (Henschel et al., 2016; Korhonen et al., 1999; Mirabel  
382 and Katz, 1974), under atmospheric conditions it may also play a negative role suppressing the

383 number concentrations of new particles by increasing aerosol surface area (Li et al. 2019).

384 Consistent with this, a negative relationship of the RH with NPF ~~probability~~frequency was found  
385 for all the sites of this study with very high  $R^2$  for almost all of them ( $R^2 > 0.80$ ). This is not simple  
386 to interpret as solar radiation intensity, temperature, RH and CS are not independent variables, since  
387 an increase in temperature of an air mass due to increased solar radiation will be associated with  
388 reduced RH, which in turn affects the CS. The sites in Greece presented lower  $R^2$  compared to the  
389 other sites while, GRERU was found to have the weakest correlation ( $R^2 = 0.22$ ). This may be due  
390 to the different seasonality of the events found for the Greek sites (being more balanced within a  
391 year), as there was increased frequency of NPF events for the seasons with higher RH compared to  
392 other sites, making it a less important factor for their occurrence as found in the previous study by  
393 Bousiotis et al., (2020). Growth rate on the other hand had a variable relationship, either positive or  
394 negative, with only a handful of background sites having strong correlations. The German  
395 background sites as well as FINRU, which were among the sites with the highest average RH  
396 (average RH for GERRU is 81.9%, GERUB is 78.7% and FINUB is 80.1%) presented a negative  
397 relationship between the RH and growth rate. DENRU (average RH at 75.7%) had a positive  
398 relationship, which might indicate that the relationship between these two variables may vary  
399 depending upon the RH range. Formation rate also appears to have a negative relationship with the  
400 RH, though this relationship was significant ( $R^2 > 0.40$ ) for only 6 sites, which once again in most  
401 cases are sites with higher RH average conditions. Along with the results of the growth rate this

402 might indicate that the RH becomes a more important factor in the development of NPF events as  
403 its values increase.

404

405 The normalised gradients once again provide some additional information. Regarding the NPF  
406 [probability frequency](#), it is found that the  $a_N^*$  was more negative at rural sites compared to roadside  
407 sites. This indicates that the RH has a smaller effect at roadside sites, as other variables, such as the  
408 atmospheric composition, are probably more important within the complex environment in this type  
409 of site. Additionally, the relationship between  $a_N^*$  and average RH at the sites had a negative  
410 relationship ( $R^2 = 0.46$ ), which further shows that the RH becomes a more important factor at  
411 higher values (Figure 4). Furthermore, at the sets of rural and roadside sites with  $R^2$  higher than  
412 0.40 for the relation between RH and the formation rate (UK and German sites), it was found that  
413 the  $a_I^*$  was more negative at the rural sites which indicates that the RH is a more important factor at  
414 rural sites compared to their respective roadside sites.

415

### 416 3.1.3 Temperature

417 Temperature can have both a direct and indirect effect in the development of NPF events, as it is  
418 directly associated with the abundance of both biogenic and anthropogenic volatile carbon, which is  
419 an important group of compounds whose oxidation products can participate in nucleation itself  
420 (Lehtipalo et al., 2018; Rose et al., 2018), as well as in the growth of newly formed particles. It may  
421 also have a negative effect on the particle size distributions or number concentrations through other

422 processes such as particle evaporation. Most of the sites of the present study presented a strong  
423 relationship of NPF [probabilityfrequency](#) with temperature, which in most cases was positive,  
424 though in many cases (such as the Danish, Finnish and Spanish sites – figures S2b, d and e) there  
425 seems to be a peak in the NPF [probabilityfrequency](#) at some temperature, after which a decline  
426 starts (though being at the higher end does not greatly affect the results). Sites with smaller  $R^2$   
427 (weaker association with temperature), were mainly those that have a seasonal variation that  
428 favoured seasons other than summer. These sites not only had weaker relationship of NPF  
429 [probabilityfrequency](#) with temperature, but in most cases had a negative relationship (background  
430 sites in Finland, Spain and Greece). The Finnish sites, having the lowest average temperatures and a  
431 sufficient amount of data below zero temperature, show at all three sites the possible presence of a  
432 peak in the NPF event [probabilityfrequency](#) for temperatures below zero (Figure S2d). This seems  
433 to be the cause of the weak relations[hips](#) found there and they seem to be associated with the  
434 formation rate  $J_{10}$ , which also seems to have an increasing trend below zero degrees (Figure S2p).  
435 This may depend on the nucleation mechanism occurring, as cluster evaporation rates of sulphuric  
436 acid clusters are sensitive to the ternary stabilising compound present (Olenius et. al., 2017), as well  
437 as the possible enhancement of growth mechanisms at lower temperatures (below 5°C) by other  
438 chemical compounds in the atmosphere (i.e. nitric acid and ammonia) as found by Wang et al.,  
439 (2020). Laboratory experiments show that the characteristics of organic aerosol forming from  
440 alpha-pinene is governed by gas phase oxidation (e.g. Ye et al. 2019). In the real atmosphere, the  
441 higher temperature enhances the amount of biogenic vapours (e.g. Paasonen et al. 2013) and,

442 although the oxidation can be more efficient at higher temperatures, the lower temperatures favour  
443 formation of more non-volatile compounds (Quéléver et al., 2019; Stolzenburg et al. 2018; Ye et al.  
444 2019).

445  
446 Growth rate had a more uniform trend, with almost all sites having a positive relationship with  
447 temperature (apart from GERRO, though with  $R^2 = 0.00$ ). This relationship was very strong for  
448 most sites ( $R^2 > 0.60$  for 10 sites), which is also confirming the summer peak found for the growth  
449 rate at most of these sites in other studies (Bousiotis et al., 2020; 2019). A rather strong relationship  
450 ( $R^2 > 0.50$ ) with temperature was also found for the formation rate for most sites, and was positive  
451 for almost all sites (apart from FINRO with  $R^2 = 0.01$  and the Greek sites with  $R^2 < 0.47$ ). As with  
452 the NPF [probabilityfrequency](#), in general the sites with a seasonal variation of events that favoured  
453 summer had the strongest relationship (high  $R^2$ ) of the temperature with formation rate, which  
454 might indicate that this variable, either through its direct or indirect effect is an important one for  
455 the seasonal variability of NPF events in a given area.

456  
457 The normalised gradients for this variable did not present a clear trend among the areas studied,  
458 other than presenting greater  $a_N^*$  for the sites with a summer peak in their NPF event seasonal  
459 variation. As with other meteorological variables, the importance of this variable became smaller  
460 with increased values in the average conditions for both the NPF [probabilityfrequency](#) (Figure 5)  
461 and  $J_{10}$ , though these relationships were not significant (biased by the very low average



temperatures and different behaviour of the variables at the Finnish sites, without which the relation<sup>ship</sup> becomes a lot clearer as indicated in Figure S13). The variation though within the sites of the same area (different sites in same country / region) appears to directly follow the variability of temperature, showing that the temperature directly affects the occurrence of NPF events when other meteorological factors remain constant, having a negative trend for all countries but Finland. The  $a_j^*$  though is found to be greater (positively or negatively) at the rural background sites than at the other two types of sites at all areas studied, showing that it is a more important factor for the formation rate at this type of site compared to others (Figure 6).

#### **3.1.4 Wind speed**

Wind speed may have both a positive and a negative effect on the occurrence of NPF events. On one hand, it may promote NPF events by the increased mixing of the condensable compounds in the atmosphere as well as by reducing the CS. On the other hand, high wind speeds may suppress NPF events due to increased dilution. It should be considered that the variability found is also affected by the specific conditions found at each site. The wind speed measurements in many cases, especially in urban sites, can be biased by the local topography or specific conditions found at each site, thus representing the local conditions for this variable rather than the regional ones. Similarly, measurements of wind speed at well sited meteorological stations may be more representative of regional conditions, than of those affecting the sites of nucleation measurement. The sites in this

482 study presented mixed results, both in the importance as well as the effect of the wind speed  
483 variability. Three different behaviours were found in the variation of NPF event  
484 [probabilityfrequency](#) and wind speed which appear to be associated with local conditions as they  
485 are almost uniformly found among the sites within close proximity. Some sites presented a steady  
486 increase of NPF event [probabilityfrequency](#) with wind speed (Danish sites, UKUB, FINRU,  
487 SPAUB and GRERU), while others were found to steadily decline with increasing wind speeds  
488 (German sites – it should be noted that the German sites are the only ones that are located at a great  
489 distance from the sea), while some were found to reach a peak and then decline, which also leads to  
490 smaller  $R^2$  (UKRU, UKRO, SPARU and to a lesser extent GREUB – figures S4a, e and f). The  
491 reasons for these differences between the sites are very hard to distinguish as apart from the wind  
492 speed the origin and the characteristics of these air masses play a crucial role. Following this, it  
493 appears that NPF [probabilityfrequency](#) is very low or zero for wind speeds close to calm for the  
494 sites with an increasing trend (as well as those that have a peak and decline after), while the  
495 opposite is observed for the German sites where the maximum NPF [probabilityfrequency](#) is found  
496 for very low wind speeds (fig. S4c).

497  
498 Similarly, the effect of different wind speeds upon the growth rate also varied a lot, though it was  
499 found to be negative in all the cases where  $R^2$  was higher than 0.50 (UKUB, DENRU, DENRO,  
500 GERRU, GERUB and GREUB). Finally, the formation rate was found to have a significant

501 correlation ( $R^2 > 0.40$ ) only at two sites (UKRO and DENRU), probably indicating that the  
502 variability of the wind speed either does not affect this variable or its effect is rather small.

503

504 The normalised gradients did not have any notable relationship to either the NPF  
505 [probabilityfrequency](#) or the formation rate further confirming that the effect of the different wind  
506 speeds is not due to its variability only, but it is also influenced by the characteristics of the  
507 incoming air masses as well as specific local conditions found at each site.

508

### 509 3.1.5 Pressure

510 In almost all the sites with available data (apart from the Spanish), the NPF [probabilityfrequency](#)  
511 presented a positive relationship with high significance at all types of sites. The greater significance  
512 found at the rural sites (apart from SPARU) indicates the increased importance of meteorological  
513 conditions in the occurrence of NPF events at this type of site. The growth rate also presented a  
514 similar picture, with positive relationships at all the background sites of this study except the ones  
515 in Greece ( $R^2 > 0.71$ ) and FINUB (though with low  $R^2$  at 0.02). This is probably associated with the  
516 seasonal variation found in Greece where higher growth rates were found in summer, a period when  
517 increased wind speeds and lower atmospheric pressure was found due to the Etesians, a pressure  
518 system that develops in the region every summer (Kalkavouras et al., 2017). An interesting finding  
519 is the negative gradients found at all the roadside sites, though the significance of these results is  
520 relatively low ( $R^2 < 0.43$ ) and always lower compared to the rural sites. The effects of pressure

521 above are not likely to be important. Once again however, this is not an independent variable and  
522 higher pressure in summer tends to be associated with higher insolation and temperatures and lower  
523 RH. Since most events occur in the warmer months of the year, this is probably the explanation for  
524 the apparent effects of pressure. The formation rate presented relationships of low significance ( $R^2$   
525  $< 0.47$ ) for the sites of this study. Due to this, pressure should not be an important factor for the  
526 formation rate at any type of site.

527

528 The normalised gradients did not present any clear trends, even for the NPF ~~probability~~frequency  
529 for which the results presented significant relationships at almost all sites.

530

## 531 **3.2 Atmospheric Composition**

532 The gradients,  $R^2$  and p-values from the analysis of a number of air pollutants ( $\text{SO}_2$ ,  $\text{NO}_x$ ,  $\text{O}_3$ ,  
533 organic compounds, sulphate and ammonia) and the CS, as well as the average conditions of these  
534 variables are found in Table 4. The results for each site and variable are found in Figures S6 – S12.

### 535 **3.2.1 Sulphur dioxide ( $\text{SO}_2$ )**

536 Sulphur dioxide, as a precursor of  $\text{H}_2\text{SO}_4$ , is considered as one of the main components associated  
537 with the NPF process. According to nucleation theories and observations,  $\text{H}_2\text{SO}_4$  is the most  
538 important compound from which the initial clusters are formed, as well as one of the candidate  
539 compounds for the initial steps of particle growth (Kirkby et al., 2011; Nieminen et al., 2010; Sipila  
540 et al., 2010; Stolzenburg et al., 2020). As  $\text{H}_2\text{SO}_4$  in the atmosphere is produced from oxidation

541 reactions of SO<sub>2</sub> it would be expected that increased concentrations of the latter would be associated  
542 with increased values for all the variables associated with the NPF process. Contrary to this though,  
543 the relationship of SO<sub>2</sub> concentrations with NPF [probabilityfrequency](#) was found to be negative at  
544 all the sites in this study with available data. [This is expected as the average concentrations of SO<sub>2</sub>](#)  
545 [on NPF event days was found to be lower compared to the average conditions in most cases as](#)  
546 [found by Bousiotis et al., \(2019; 2020\).](#) This relationship was relatively strong ( $R^2 > 0.50$ ) in most  
547 areas with an increased significance at roadside sites compared to their respective rural sites. As this  
548 is a negative relationship, this may indicate that SO<sub>2</sub> is in sufficient concentrations for H<sub>2</sub>SO<sub>4</sub>  
549 formation, thus not suppressing the occurrence of NPF events, as well as showing that in increased  
550 concentrations, it is a more important factor (or surrogate for a factor) in preventing the occurrence  
551 of NPF events within the urban environment, as higher SO<sub>2</sub> is likely associated with increased co-  
552 emitted particle pollution and hence CS. The growth rate on the other hand, presented mixed results  
553 and the significance of the relationships is low in most cases, which makes these results unreliable.  
554 Finally, the relationship of SO<sub>2</sub> concentrations with the formation rate was found to be positive at  
555 all sites but SPARU and FINRU (which had the lowest concentrations across the sites with  
556 available data). The significance of this relationship was rather low ( $R^2 < 0.40$ ) for all but the  
557 roadside sites. This suggests that higher H<sub>2</sub>SO<sub>4</sub> concentrations favour greater formation rates (i.e.  
558 more particles can be formed), rather than necessarily promoting nucleation itself because of the  
559 competing effect of condensation onto the pre-existing particle population.

560

561 The normalised gradients  $a_N^*$  were found to be more negative at the background sites compared to  
562 their respective roadside sites, as well as being less negative in the UK (where  $SO_2$  is in greater  
563 abundance) compared to the other sites with relatively significant relationships. Plotting the average  
564  $SO_2$  concentrations with the normalised gradients  $a_N^*$  for the all sites (though not all had significant  
565 relationships), a positive relationship with relatively high  $R^2$  (when the extreme values from  
566 Marylebone Road-UKRO are removed) is found which might indicate that while increased  
567 concentrations are a negative factor in NPF event occurrence at a given site, in general the sites with  
568 higher  $SO_2$  concentrations on average present higher [probabilityfrequency](#) for NPF events (Figures  
569 7a and 7b). This appears to be in agreement with Dall'Osto et al. (2018) who discussed the variable  
570 role of  $SO_2$  depending on its concentrations. [Similar findings for the effect of  \$SO\_2\$  were also found](#)  
571 [in previous worksstudies \(Jung et al., 2006; 2008\), relating particle acidity to NPF. Finally, nNo](#)  
572 significant relationships were found for the values of  $a_j^*$  as in most cases these relationships were  
573 rather weak.

574

### 575 3.2.2 Nitrogen oxides or nitrogen dioxide ( $NO_x$ or $NO_2$ )

576  $NO_x$  and  $NO_2$  are directly associated with pollution, which can be a limiting factor for NPF events  
577 as it increases the CS and may suppress the events (An et al., 2015), though with the reduction of  
578  $SO_2$  concentrations achieved the last couple of decades, there is a possibility for oxidation products  
579 of  $NO_x$  to become an important component for NPF (Wang et al., 2020). For almost all sites (apart  
580 from GRERU) with available data a negative relationship between the NPF [probabilityfrequency](#)

581 and NO<sub>x</sub> concentrations (or NO<sub>2</sub> depending on the available data) was found. Similarly, for all the  
582 sites but SPARU and GRERU, the correlations were ~~strong~~relatively strong with  $R^2 > 0.43$ . The  
583 rural background sites had a weaker relationship between the two variables compared to the urban  
584 sites, which is probably associated with them having rather low concentrations and variability of  
585 NO<sub>x</sub> (or NO<sub>2</sub>), making the variations of this factor less important. Growth rate had weaker  
586 correlations with NO<sub>x</sub> and different trends between the sites, either being positive or negative. The  
587 variable effect of NO<sub>x</sub> on particle growth, shifting HOMs volatility, was previously discussed by  
588 Yan et al. (2020). While variability was found for the background sites, all roadside sites regardless  
589 of the strength of the relationship had a positive relationship between NO<sub>x</sub> and the growth rate. This  
590 may indicate the different components associated with the growth process at each type of site  
591 which, as found in other studies, can be related to compounds associated with combustion processes  
592 that take place within the urban environment (Guo et al., 2020; Wang et al., 2017a). The formation  
593 rate presents few cases of strong relationships, with variable trends (positive and negative). While  
594 much effort was made to isolate the effect of NPF events by taking a shorter time frame before the  
595 event, the effect of local pollution is still included, especially at the urban sites (which probably  
596 explains the positive effect found).

597

598 The normalised gradients do not provide a significant result for the relationship of this variable with  
599 either the probability~~frequency~~ of the events or the formation rate. The only noteworthy points are  
600 the more negative  $a_N^*$  at the rural background sites compared to the roadside sites in all the areas

601 studied, which shows the increased importance of a clean environment for NPF events to occur in  
602 areas where condensable compounds are in lesser abundance, such as a rural environment.  
603 Additionally, the negative gradients found at all the roadside sites, which increases the confidence  
604 that the events extracted at the roadside sites are not pollution incidents but NPF events. However,  
605 it appears that traffic pollution favours higher particle growth rates, although the components  
606 responsible for this effect are unknown.

607

### 608 3.2.3 Ozone (O<sub>3</sub>)

609 Ozone is typically the result of atmospheric photochemistry and is itself a source of hydroxyl  
610 radical through photolysis, or ozonolysis of alkenes both during daytime and night-time (Fenske et  
611 al., 2000). It might therefore be expected to act as an indicator of photochemical activity which  
612 promotes the oxidation of SO<sub>2</sub> and VOCs. Ozone concentrations may be directly related to the  
613 solar radiation intensity as well as the pollution levels in the area studied, and O<sub>3</sub> is considered as a  
614 positive factor in the occurrence of NPF events (Woo et al., 2001; Berndt et al., 2006). As with the  
615 solar radiation intensity, there is a strong relationship between O<sub>3</sub> concentration and the  
616 [probability/frequency](#) for NPF events. This positive relationship, [which is in agreement with the](#)  
617 [higher concentrations of O<sub>3</sub> found on NPF event days compared to average conditions for all sites in](#)  
618 [Bousiotis et al., \(2019; 2020\)](#), was found to be stronger for the sites in northern Europe ( $R^2 > 0.51$ ),  
619 while it was not significant ( $R^2 < 0.38$ ) for the sites in southern Europe (Spanish sites and GRERU),  
620 possibly indicating that O<sub>3</sub> is a less important factor at the southern sites. Specifically for the



621 Spanish sites which have the highest average concentrations of O<sub>3</sub> with some extreme values  
622 (Querol et al., 2017), the relationship of O<sub>3</sub> concentrations with the NPF ~~probability~~frequency  
623 presents a unique trend (Figure S8d), having a clear peak then a steady decline at both sites (though  
624 at different O<sub>3</sub> concentrations), which is also responsible for the low correlations found (this trend  
625 seems to also occur at SPARU for the growth rate and to a lesser extent for the formation rate as  
626 well, though for different O<sub>3</sub> concentration ranges – figures S8i and n). The specific variability  
627 found at the Spanish sites was also studied by Carnerero et al., (2019). For sites with a marked  
628 seasonal variation in ozone, associations with NPF may be artefactual due to correlations with other  
629 variables such as temperature, RH and solar radiation intensity.

630  
631 Unlike the solar radiation intensity though, the growth rate presents a negative relationship at the  
632 sites where the relationship between these two variables was significant (UKRU, UKUB, DENUB  
633 and FINRU), which might either be an indication of a polluted background that may have a  
634 negative effect in the growth of the newly formed particles (though the trends found for NO<sub>x</sub>  
635 indicate differently) or specific chemical processes which cannot be identified due to the lack of  
636 detailed chemical composition data. A significant relationship between O<sub>3</sub> and the formation rate  
637 was only found for two sites (UKRO and DENRO, though the trends become a lot clearer if some  
638 values are removed from the extreme lower or higher end). This way the relationships become  
639 strong, but positive, for some areas and negative for some others without any clear trend (type or  
640 location of the site, O<sub>3</sub> concentrations etc.). No clear relationship between these two variables was

641 found as the sites with strong relationship have both positive (DENRO) and negative (UKRO)  
642 relationships and as a result no confident conclusions can be drawn.  
643 As the correlations found were strong the normalised gradients for NPF [probabilityfrequency](#), when  
644 plotted against the average concentrations of O<sub>3</sub>, present a negative correlation with relatively high  
645 R<sup>2</sup> (0.64), indicating that the O<sub>3</sub> is a more important factor in the occurrence of NPF events when in  
646 lower concentrations (Figure 8). Finally, though with a low level of confidence for the southern  
647 sites, the a<sub>N</sub><sup>\*</sup> were smaller at the southern sites compared to those in the north, up to one order of  
648 magnitude between FINRU (furthest north rural background) and GRERU (furthest south rural  
649 background).

650

### 651 **3.2.4 Organic compounds**

#### 652 **3.2.4.1 Particulate organic carbon (OC)**

653 Organic carbon (OC) compounds in the secondary aerosol typically enter the particles via  
654 condensational processes, with a role that becomes increasingly important as the size of the  
655 particles becomes larger (Nieminen et al., 2010; Zhang et al., 2012; Shrivastava et al., 2017).  
656 Particulate OC, the data for which is available in the present study, can be associated with pollution,  
657 especially in the urban environment. Only a few of the sites of the present study were found to have  
658 a relatively strong negative relationship (R<sup>2</sup> > 0.50) of particulate OC with the NPF  
659 [probabilityfrequency](#) (UKUB, UKRO and DENRU). Regardless though of the strength of this  
660 relationship, all other sites (apart from FINRU) had a negative relationship between these two

661 variables as well, consistent with increased concentrations of particulate OC being associated with  
662 increased pollution, which elevate the CS, suppressing the occurrence of NPF events. Growth rate  
663 on the other hand was found to have a positive relationship ( $R^2 > 0.40$ ) for most of the sites. This  
664 relationship appeared to be stronger (higher  $R^2$ ) at the roadside sites with available data compared  
665 to their respective rural background sites. The relationship between particulate OC and the growth  
666 rate was positive at all the sites with available data regardless of their significance showing that,  
667 despite its effect in the occurrence of NPF events, it is still a favourable variable for the growth of  
668 the particles. The formation rate was found to have a significant relationship with particulate OC  
669 concentrations at half of the sites with available data (UKUB, UKRO, DENRU, DENRO).

670  
671 The normalised gradients for this variable did not present any noteworthy relationships with either  
672 the type of site or the concentrations of OC at a given site.

673

#### 674 3.2.4.2 Volatile organic compounds (VOCs)

675 Many volatile organic compounds have been found to be associated with the NPF process. Benzene,  
676 toluene, ethylbenzene, m-p-xylene, o-xylene and trimethylbenzenes have been reported to be able to  
677 form Highly Oxygenated Organic Molecules (HOMs) in flow tubes (Wang et al., 2017a; Molteni et  
678 al., 2018), which may act as contributors to particle nucleation and/or growth. Xylenes, and to a  
679 lesser extent trimethylbenzenes, are the most efficient at forming HOMs. Benzene and toluene are  
680 less efficient and will form more volatile HOMs. These HOMs may all be too volatile to form new

681 particles, though this is not yet confirmed. Chamber studies involving  $\text{H}_2\text{SO}_4$  and trimethylbenzene  
682 oxidation products were associated with high formation rates when measuring  $\text{J}_{1.5}$  (Metzger et al.,  
683 2010). All these HOMs though will be sufficiently involatile to contribute to particle growth. Those  
684 with higher oxygen content or carbon number will be classed as LVOC and if they dimerise, they  
685 will form ELVOC (Bianchi et al., 2019). Monoterpenes can also form HOMs which drive both the  
686 formation (Ehn et al., 2014; Riccobono et al., 2014) and growth (Tröstl et al., 2016), while isoprene  
687 can act as a sink for hydroxyl radical (Kiendler-Scharr et al., 2009) and is not as effective in HOM  
688 and secondary organic aerosol formation compared to monoterpenes (McFiggans et al., 2019).  
689  
690 Volatile organic compound data were available for three of the sites of this study (Table S2). Two  
691 of the sites with VOC data were from the rural background and the roadside site in the UK. Most of  
692 the compounds are associated with combustion sources and were found to have a negative  
693 relationship with NPF event occurrence at both sites, with high  $R^2$  ( $R^2 > 0.50$ ) in most cases.  
694 Additionally, isoprene, which may have either biogenic or anthropogenic sources (Wagner and  
695 Kuttler, 2014) was also found to have a negative relationship with NPF event occurrence at  
696 Marylebone Road-UKRO, though with low  $R^2$  (0.07). This result is in line with the VOCs being  
697 strongly correlated with particulate OC (which presented a negative relationship with NPF event  
698 [probabilityfrequency](#), as discussed in Section 3.2.4.1), as well as with the CS (which also presented  
699 a negative relationship with NPF event [probabilityfrequency](#), as mentioned in Section 3.2.6), further  
700 associating these compounds with combustion emissions.

701

702 Growth rate was found to have a positive relationship with VOCs in almost all cases for both UK  
703 sites. Few exceptions were found (with only 1,3 butadiene having a relatively high  $R^2$ ) which  
704 presented a negative relationship with the growth rate in rural Harwell-UKRU. Finally, the  
705 formation rate presented a different behaviour between the two sites. At UKRU, the relationship  
706 was unclear in most cases, with a group of VOCs presenting a negative relationship with the  
707 formation rate (ethane, ethene, propane, 1,3 butadiene, toluene, ethylbenzene, o-xylene and 1,2,4  
708 trimethylbenzene – with  $R^2 > 0.40$ ), two VOCs presented a rather clear positive relationship with  
709 the formation rate (iso-pentane and 2-methylbenzene) and the rest of the VOCs had an unclear  
710 relationship. At UKRO though, VOCs presented a positive relationship with the formation rate (for  
711 particles of diameter 16 nm). This is probably due to the fact that these VOCs are associated with  
712 pollution emissions (as mentioned earlier) and though a smaller time window was chosen to avoid  
713 including the effect of the morning rush hour traffic, this is very difficult in the traffic polluted  
714 environment of Marylebone Road.

715

716 As Hyytiälä (FINRU) is a rural background site far from the direct effect of combustion emissions,  
717 different VOCs were measured, which mainly originate from biogenic sources rather than  
718 anthropogenic ones. The results were mixed and less clear compared to those from the UK sites  
719 (mainly due to the smaller dataset), and three groups were found depending on their relationship  
720 with NPF [probabilityfrequency](#). The first group, including acetonitrile, acetic acid and methyl ethyl

ketone (MEK) presented a slight positive relationship. The second group presented a negative relationship, with the VOCs in this group being monoterpenes, methacroleine, benzene, isoprene and toluene (only the last two have  $R^2 > 0.50$ ). Finally, the third group included VOCs that presented a peak and then a decline for higher concentrations including methanol, and acetone. Two groups of VOCs were found depending on their relationship with the growth rate. The ones with a positive relationship being methanol, acetonitrile, acetone, acetic acid, isoprene, methacroleine, monoterpenes and toluene, while acetaldehyde, MEK and benzene had a negative relationship, with relatively high  $R^2$  in most cases. Finally, the results with the formation rate were unclear with only a handful presenting weak ( $R^2 < 0.21$ ) positive (methanol, acetic acid and benzene) or negative (MEK) relationships that do not appear to be significant. The normalised gradients cannot be used for VOCs as there are very few sites with available data.

### **3.2.5 Sulphate ( $\text{SO}_4^{2-}$ )**

Sulphate ( $\text{SO}_4^{2-}$ ) is a major secondary constituent of aerosols. Secondary  $\text{SO}_4^{2-}$  aerosols largely arise from either gas phase reaction between  $\text{SO}_2$  and OH, or in the aqueous phase by the reaction of  $\text{SO}_2$  and  $\text{O}_3$  or  $\text{H}_2\text{O}_2$ , or  $\text{NO}_2$  (Hidy et al., 1994). In environments where  $\text{SO}_4^{2-}$  chemistry is dominant (i.e. remote areas),  $\text{SO}_4^{2-}$  and ammonium (bi) sulphate ( $(\text{NH}_4)_2\text{SO}_4$  and  $\text{NH}_4\text{HSO}_4$ ) particles are a large relative contributor to aerosol mass, while this contribution is lower in environments where other emissions are also significant (i.e. urban areas where the secondary  $\text{NO}_3^-$  relative contribution is a lot higher). While not well established, a possible relationship of  $\text{SO}_4^{2-}$ -containing compounds

741 and variables of NPF events was found in previous studies (Beddows et al., 2015; Minguillón et al.,  
742 2015; Wang et al., 2017b). In the present study, only a few sites had  $\text{SO}_4^{2-}$  data available, for  $\text{PM}_{10}$   
743 ( $\text{FINRU}$ ),  $\text{PM}_{2.5}$  (Danish sites) or  $\text{PM}_{10}$  (rest of the sites). While this data cannot be considered as  
744 directly associated with the ultrafine particles, for two sites with available [AMS-ACSM](#) data for  
745 ultrafine particles, the direct comparison between  $\text{SO}_4^{2-}$  aerosol in PM and in the range of particles  
746 of about 50 nm, very high correlations were found (results not included). For all the sites with  
747 available data the NPF [probability frequency](#) presented a negative relationship. The significance of  
748 this relationship was found to be relatively high ( $R^2 > 0.50$ ) only for background sites (apart from  
749  $\text{GERRU}$ , which has rather low concentrations and probably different mechanisms for the NPF  
750 events). Similarly, the growth rate presented a significant relationship ( $R^2 > 0.40$ ) for the same  
751 background sites (apart from  $\text{FINRU}$ ), though this relationship was found to be positive at all sites  
752 regardless of its significance. Finally, the formation rate did not present a clear trend as it was found  
753 to have both negative and positive relationships for different sites. This relationship was significant  
754 only for two rural sites ( $\text{UKRU}$  and  $\text{DENRU}$ ) and as a result no conclusions can be reached.

755

756 The normalised gradients cannot be used for any analysis on sulphate as the measurements available  
757 are from different particle size ranges.

758

### 759 3.2.6 Gaseous ammonia ( $\text{NH}_3$ )

Ammonia (NH<sub>3</sub>) can be an important compound in the nucleation process according to the ternary theory (Kirkby et al., 2011; Napari et al., 2002). It was found that elevations in NH<sub>3</sub> concentrations can lead to elevations to NPF rate (Lehtipalo et al., 2018) and it was also found to be an important factor for NPF event occurrence even when stronger bases are present in high concentrations (Glasoe et al., 2015). No significant variation was found though between event and non-event days in a previous study in Harwell - UKRU (Bousiotis et al., 2019). Data for gaseous ammonia was only available for UKRU and presented a positive relationship with NPF [probabilityfrequency](#), until reaching a peak point. Further increase in NH<sub>3</sub> concentrations presented a decline with NPF [probabilityfrequency](#) (Figure S11a), which might be due to its association with increased pollution levels. It presented a clear positive relationship with both the growth rate (though it also appears to decline at high concentrations) and the formation rate, consistent with its well-established role in accelerating both of these processes (Kirkby et al. 2011; Stolzenburg et al., 2020).

772

### 773 3.2.7 Condensation sink (CS)

The CS is a measure of the rate at which molecules will condense onto pre-existing aerosols (Lehtinen et al., 2003). It is highly dependent on the number and size of the particles in the atmosphere and as a result it is expected to be affected by both the local emissions within the urban environment as well as the formation and growth of the particles due to NPF events. As a result, for the specific metric a time frame before the events are in full development was chosen (05:00 to 10:00 LT) to avoid including the effect of the NPF events and provide a picture of the atmospheric



780 conditions that preceded the NPF events. With this data, the NPF [probabilityfrequency](#) presented  
781 very strong relationships with the condensation sink. Two groups of sites were found though; those  
782 which had a positive relationship and those with a negative relationship. In the first group are the  
783 sites in Germany and Greece while all others had a negative relationship. This grouping follows the  
784 trend between the countries, the sites of which presented a greater or smaller CS on NPF event days  
785 [according to the findings in Bousiotis et al., \(2019; 2020\)](#) (having positive or negative gradients  
786 respectively), though it is unknown what causes this behaviour (at the German sites and GREUB it  
787 may be associated with the very high formation rates on NPF event days). While the gradients from  
788 this analysis cannot be used for direct comparisons, a trend was found for which the gradients were  
789 more positive or negative at the rural sites compared to their respective roadside sites, which might  
790 indicate the greater importance of the variability of the CS at the rural sites in the occurrence of  
791 NPF events.

792  
793 The growth rate was positively correlated with the CS for most of the sites, with [strong-relatively](#)  
794 [strong](#) relationships ( $R^2 > 0.40$ ) for about half of them. As the CS is a metric of pre-existing  
795 particles, it is also associated with the level of pollution in a given area. The increased significance  
796 and gradient found at the rural sites probably indicates the importance of enhanced presence of  
797 condensable compounds in a cleaner environment, which in many cases are associated with the  
798 moderate presence of pollution. The formation rate was also found to have a positive relationship  
799 with the CS. This relationship was more significant at the roadside sites of this study, a result which

800 to some extent is biased by the presence of increased traffic emissions found in the timeframe  
801 chosen. While to an extent, increased presence of condensable compounds can be favourable for  
802 greater formation rates, this result should be considered with great caution.

803

804 The normalised gradients  $a_N^*$  followed a similar trend as those found with the initial analysis. These  
805 gradients were found to be more positive or negative, depending on the trend of the given area, at  
806 the rural sites compared to their roadside sites. The urban background sites did not always have a  
807 uniform behaviour (though in UK, Denmark and Finland these were between the rural site and the  
808 roadside site), due to their more diverse character compared to the other two types of sites.

809

### 810 **3.3 Association of the Effect of the Variables**

811 The Pearson correlation coefficients for the variables studied on each site are found in Table S1.

812 The relatively strong relationship between the solar radiation intensity, temperature and  $O_3$  found,  
813 as well as their anticorrelation with the RH may lead to the conclusion that not all these factors play  
814 a role in NPF events, but their visible effect is the result of their relationship with each other. There  
815 is a similar case with the association of the CS and  $NO_x$  (or  $NO_2$ ), and OC, as well as  $SO_2$ ,  
816 especially at urban sites. However, the factors affect different outcomes differently, as for example  
817 the solar radiation intensity does not seem to be as important a factor for the growth rate as  
818 temperature, or  $O_3$  does not seem to be strongly associated with either the formation or the growth  
819 rate. This is further established by the fact that some of these variables do not correlate well at the

southern sites, but still appear to be associated with either the [probabilityfrequency](#) of NPF events or the growth or nucleation rate. The effects of all of these factors have been demonstrated in both laboratory and atmospheric studies in the past and were discussed earlier in this paper. By the analysis provided in the present study, the effect of each of these variables is further established, providing an association of each one of these variables with either the formation or the growth mechanism. However, RH does not seem to be a consistent factor in any mechanism, and it appears that its effect is dependent on location specific conditions, although it was the variable with the most consistent relation with NPF event [probabilityfrequency](#) at almost all sites.

### **3.4 Relationship to a previous multi-station European study**

The findings of our study in respect of the background sites show many similarities with the conclusions drawn in the previous multi-station study in Europe by Dall'Osto et al. (2018) despite the two studies using several different sampling stations as well as some in common. Both studies point towards the influence of variables such as solar radiation intensity and CS upon the occurrence of NPF events. The previous study suggested that different compounds participate in the growth of the particles, depending on the area considered. Thus, for northern and southern sites the growth of the particles is suggested to be driven mainly by organic compounds, while for the sites in central Europe sulphate plays a more important role. These findings are confirmed by the present study, as the growth rate was found to correlate better with organic compounds for the rural sites in Finland and Greece, while  $\text{SO}_4^{2-}$  presented a stronger relationship with the growth rate for the

840 Danish and German sites (the latter presented high gradient values but low  $R^2$  due to a decline at  
841 higher  $\text{SO}_4^{2-}$  concentrations – figure S10i, probably associated with NPF events being suppressed  
842 by increased pollution). The growth of the particles at the rural background site in the UK,  
843 characterised as “Overlap” in the previous study, was found to be strongly associated with both  
844 organic compounds and sulphate, consistent with it being in the central group.

845  
846 The seasonality of NPF events at northern sites was hard to explain in the previous study, and the  
847 possible effect of low temperature was considered. In the present study, the Finnish background  
848 sites presented a double-peak relationship of NPF [probabilityfrequency](#) with temperature, with one  
849 of the peaks being below zero degrees. This might point to the possibility of different compounds  
850 driving the events for different temperature ranges, as well as the increased nucleation rate of  
851  $\text{H}_2\text{SO}_4$  at lower temperatures (Kirkby et al., 2011; Yan et al., 2018), which makes the occurrence of  
852 NPF events more probable at lower temperatures in a region with low  $\text{SO}_2$  concentrations.

853

#### 854 4. CONCLUSIONS

855 The present study attempts to explain the effect of several meteorological and atmospheric variables  
856 on the occurrence and development of NPF events, by using a large-scale dataset. More than 85  
857 site-years of data from 16 sites from six countries in Europe were analysed for NPF events. A total  
858 of 1952 NPF events with consequent growth of the newly formed particles were extracted and with  
859 the use of binned linear regression, the relationship between three variables associated with NPF

860 events (NPF event [probabilityfrequency](#), formation and growth rate) with meteorological conditions  
861 and atmospheric composition was studied. Among the meteorological conditions, solar radiation  
862 intensity, temperature and atmospheric pressure presented a positive relationship with the  
863 occurrence of NPF events [in the majority of the sites \(though exceptions were found as well, mostly](#)  
864 [in the southern sites\)](#), either promoting the formation or growth rate. RH presented a negative  
865 relationship with NPF event [probabilityfrequency](#) which in most cases was associated with it being  
866 a limiting factor on particle formation at higher average values. Wind speed on the other hand  
867 presented variable results, appearing to depend on the location of the sites rather than their type.  
868 This shows that while wind speed can be a factor in NPF event occurrence, the origin of the  
869 incoming air masses also plays a very important role. In most cases, meteorological conditions,  
870 such as temperature or RH appeared to be more important factors in NPF event occurrence at rural  
871 sites compared to urban sites, suggesting that NPF events are driven more by them at this type of  
872 site compared to urban environments and the more complex chemical interactions found there.  
873 Additionally, while some meteorological variables appeared to play a crucial role in the occurrence  
874 of NPF events, this role appears to become less important at higher values when a positive relation  
875 was found (or lower when a negative relation was found).

876

877 The results for the levels of atmospheric pollutants presented a more interesting picture as most of  
878 these, which appear to be either directly or indirectly associated with the NPF process were found to  
879 have negative relationships with NPF [probabilityfrequency](#). This is probably due to the fact that

880 increased concentrations of such compounds are associated with more polluted conditions, which  
881 are a limiting factor in the occurrence of NPF events, as was found with the negative relationship  
882 between the CS and NPF [probabilityfrequency](#) in most cases. Thus, SO<sub>2</sub>, NO<sub>x</sub> (or NO<sub>2</sub>), particulate  
883 OC and SO<sub>4</sub><sup>2-</sup> concentrations were negatively correlated with NPF [probabilityfrequency](#) in most  
884 cases. Average SO<sub>2</sub> concentrations appeared to correlate positively with the normalised NPF event  
885 [probabilityfrequency](#) gradients with a relatively significant correlation, indicating that while  
886 increasing concentrations have a negative impact in the occurrence of NPF events at a given site, in  
887 general sites with higher SO<sub>2</sub> concentrations have higher [probabilityfrequency](#) for NPF events.  
888 Conversely, these compounds in many cases had a positive relationship (not always though with  
889 high significance) with the other variables considered. Thus, particulate OC (and VOCs where data  
890 was available) and SO<sub>4</sub><sup>2-</sup> consistently had a positive relationship with the growth rate, while SO<sub>2</sub>  
891 was positively associated with both the formation and growth rate in most cases. Finally, O<sub>3</sub> was  
892 positively correlated with NPF event [probabilityfrequency](#) at all sites in this study, though it  
893 presented variable results with the other two variables. As with some meteorological conditions it  
894 was found that at sites with increased concentrations of O<sub>3</sub>, its importance as a factor was  
895 decreased, which to some extent can be related with the high CS associated with peak summer O<sub>3</sub>  
896 days in southern Europe.

897

898 It should be noted that the variables considered are in many cases inter-related (e.g. temperature and  
899 RH) and this considerably complicates the interpretation in terms of causal factors. Large datasets

900 are very useful in providing more uniform results by removing the possible bias of short period  
901 extremities, which may lead to wrong assumptions. This study, apart from providing insights into  
902 the effect of a number of variables on the occurrence and development of NPF events in  
903 atmospheric conditions across Europe, also shows the differences that climatic, land use and  
904 atmospheric composition variations cause to those effects. Such variations are probably the cause of  
905 the differences found among previous studies. Following from this, the importance of a high-  
906 resolution measurement network, both spatially and temporally is underlined, as it can help in  
907 elucidating the mechanisms of new particle formation in the real atmosphere.

908

#### 909 **DATA ACCESSIBILITY**

910 Data supporting this publication are openly available from the UBIRA eData repository at

911 <https://doi.org/10.25500/edata.bham.00000491>.~~https://doi.org/~~

912

#### 913 **AUTHOR CONTRIBUTIONS**

914 The study was conceived and planned by RMH who also contributed to the final manuscript, and  
915 DB who also carried out the analysis and prepared the first draft of the manuscript. AM, JKN, CN,  
916 JVN, HP, NP, AA, GK, SV and KE have provided with the data for the analysis. JB provided help  
917 with analysis of the data. FDP provided advice on the analysis. MDO, XQ and TP contributed to the  
918 final manuscript.

919

920 **COMPETING INTERESTS**

921 The authors have no conflict of interests.

922

923 **ACKNOWLEDGMENTS**

924 This work was supported by the National Centre for Atmospheric Science funded by the U.K.

925 Natural Environment Research Council (R8/H12/83/011).

926



## 927 REFERENCES

- 928
- 929 Aalto, P., Hämeri, K., Becker, E. D. O., Weber, R., Salm, J., Mäkelä, J. M., Hoell, C., O'Dowd, C.  
 930 D., Karlsson, H., Hansson, H., Väkevä, M., Koponen, I. K., Buzorius, G. and Kulmala, M.: Physical  
 931 characterization of aerosol particles during nucleation events, *Tellus, Ser. B Chem. Phys. Meteorol.*,  
 932 53(4), 344–358, doi:10.3402/tellusb.v53i4.17127, 2001.
- 933
- 934 Alam, A., Shi, J. P. and Harrison, R. M.: Observations of new particle formation in urban air, *J.*  
 935 *Geophys. Res. Atmos.*, 108(D3), n/a-n/a, doi:10.1029/2001JD001417, 2003.
- 936
- 937 An, J., Wang, H., Shen, L., Zhu, B., Zou, J., Gao, J. and Kang, H.: Characteristics of new particle  
 938 formation events in Nanjing, China: Effect of water-soluble ions, *Atmos. Environ.*, 108, 32–40,  
 939 doi:10.1016/j.atmosenv.2015.01.038, 2015.
- 940
- 941 Bae, M.-S., Schwab, J. J., Hogrefe, O., Frank, B. P., Lala, G. G. and Demerjian, K. L.:  
 942 Characteristics of size distributions at urban and rural locations in New York, *Atmos. Chem. Phys.*  
 943 *Discuss.*, 10(1), 69–108, doi:10.5194/acpd-10-69-2010, 2010.
- 944
- 945 Beddows, D. C. S., Harrison, R. M., Green, D. C. and Fuller, G. W.: Receptor modelling of both  
 946 particle composition and size distribution from a background site in London, UK, *Atmos. Chem.*  
 947 *Phys.*, 15(17), 10107–10125, doi:10.5194/acp-15-10107-2015, 2015.
- 948
- 949 [Beddows, D. C. S. and Harrison, R. M.: Receptor modelling of both particle composition and size](#)  
 950 [distribution from a background site in London , UK – a two-step approach', pp. 4863–4876, 2019.](#)
- 951
- 952
- 953 Berland, K., Rose, C., Pey, J., Culot, A., Freney, E., Kalivitis, N., Kouvarakis, G., Cerro, J. C., Mallet,  
 954 M., Sartelet, K., Beckmann, M., Bourriane, T., Roberts, G., Marchand, N., Mihalopoulos, N. and  
 955 Sellegri, K.: Spatial extent of new particle formation events over the Mediterranean Basin from  
 956 multiple ground-based and airborne measurements, *Atmos. Chem. Phys.*, 17(15), 9567–9583,  
 957 doi:10.5194/acp-17-9567-2017, 2017.
- 958
- 959 Berndt, T., Böge, O. and Stratmann, F.: Formation of atmospheric H<sub>2</sub>SO<sub>4</sub>H<sub>2</sub>O particles in the  
 960 absence of organics: A laboratory study, *Geophys. Res. Lett.*, 33(15), 2–6,  
 961 doi:10.1029/2006GL026660, 2006.
- 962
- 963 Bianchi, F., Kurtén, T., Riva, M., Mohr, C., Rissanen, M. P., Roldin, P., Berndt, T., Crounse, J. D.,  
 964 Wennberg, P. O., Mentel, T. F., Wildt, J., Junninen, H., Jokinen, T., Kulmala, M., Worsnop, D. R.,  
 965 Thornton, J. A., Donahue, N., Kjaergaard, H. G. and Ehn, M.: Highly oxygenated organic molecules  
 966 (HOM) from gas-phase autoxidation involving peroxy radicals: A key contributor to atmospheric

967 aerosol, *Chem. Rev.*, 119, 3472–3509, doi:10.1021/acs.chemrev.8b00395, 2019.  
968  
969 Bigi, A. and Harrison, R. M.: Analysis of the air pollution climate at a central urban background site,  
970 *Atmos. Environ.*, 44(16), 2004–2012, doi:10.1016/j.atmosenv.2010.02.028, 2010.  
971  
972 Birmili, W., Weinhold, K., Rasch, F., Sonntag, A., Sun, J., Merkel, M., Wiedensohler, A., Bastian,  
973 S., Schladitz, A., Löschau, G., Cyrus, J., Pitz, M., Gu, J., Kusch, T., Flentje, H., Quass, U., Kaminski,  
974 H., Kuhlbusch, T. A. J., Meinhardt, F., Schwerin, A., Bath, O., Ries, L., Wirtz, K. and Fiebig, M.:  
975 Long-term observations of tropospheric particle number size distributions and equivalent black  
976 carbon mass concentrations in the German Ultrafine Aerosol Network (GUAN), *Earth Syst. Sci. Data*,  
977 8(2), 355–382, doi:10.5194/essd-8-355-2016, 2016.  
978  
979 Bousiotis, D., Pope, F. D., Beddows, D. C., Dall’Osto, M., Massling, A., Nøjgaard, J. K.,  
980 Nørdestrom, C., Niemi, J. V., Portin, H., Petäjä, T., Perez, N., Alastuey, A., Querol, X., Kouvarakis,  
981 G., Vratolis, S., Eleftheriadis, K., Wiedensohler, A., Weinhold, K., Merkel, M., Tuch, T., and  
982 Harrison, R. M.: An Analysis of New Particle Formation (NPF) at Thirteen European Sites, *Atmos.*  
983 *Chem. Phys. Discuss.*, <https://doi.org/10.5194/acp-2020-414>, in review, 2020.  
984  
985 Bousiotis, D., Osto, M., Beddows, D. C. S., Pope, F. D. and Harrison, R. M.: Analysis of new  
986 particle formation (NPF) events at nearby rural, urban background and urban roadside sites, *Atmos.*  
987 *Chem. Phys.*, 19, 5679–5694, 2019.  
988  
989 Brines, M., Dall’Osto, M., Beddows, D. C. S., Harrison, R. M., Gómez-Moreno, F., Núñez, L.,  
990 Artíñano, B., Costabile, F., Gobbi, G. P., Salimi, F., Morawska, L., Sioutas, C. and Querol, X.: Traffic  
991 and nucleation events as main sources of ultrafine particles in high-insolation developed world cities,  
992 *Atmos. Chem. Phys.*, 15(10), 5929–5945, doi:10.5194/acp-15-5929-2015, 2015.  
993  
994 Carnerero, C., Pérez, N., Petäjä, T., Laurila, T. M., Ahonen, L. R., Kontkanen, J., Ahn, K. H.,  
995 Alastuey, A. and Querol, X.: Relating high ozone, ultrafine particles, and new particle formation  
996 episodes using cluster analysis, *Atmos. Environ. X*, 4(October), doi:10.1016/j.aeaoa.2019.100051,  
997 2019.  
998  
999 Charron, A. and Harrison, R. M.: Primary particle formation from vehicle emissions during exhaust  
1000 dilution in the roadside atmosphere, *Atmos. Environ.*, 37(29), 4109–4119, doi:10.1016/S1352-  
1001 2310(03)00510-7, 2003.  
1002  
1003 Charron, A., Birmili, W. and Harrison, R. M.: Fingerprinting particle origins according to their size  
1004 distribution at a UK rural site, *J. Geophys. Res. Atmos.*, 113(7), 1–15, doi:10.1029/2007JD008562,  
1005 2008.  
1006

1007 Charron, A., Degrendele, C., Laongsri, B. and Harrison, R. M.: Receptor modelling of secondary and  
 1008 carbonaceous particulate matter at a southern UK site, *Atmos. Chem. Phys.*, 13(4), 1879–1894,  
 1009 doi:10.5194/acp-13-1879-2013, 2013.  
 1010  
 1011 Cheung, H. C., Chou, C. C.-K., Huang, W.-R. and Tsai, C.-Y.: Characterization of ultrafine particle  
 1012 number concentration and new particle formation in an urban environment of Taipei, Taiwan, *Atmos.*  
 1013 *Chem. Phys.*, 13(17), 8935–8946, doi:10.5194/acp-13-8935-2013, 2013.  
 1014  
 1015 Chu, B., Kerminen, V., Bianchi, F., Yan, C., Petäjä, T. and Kulmala, M.: Atmospheric new particle  
 1016 formation in China, *Atmos. Chem. Phys.*, 19, 115–138, doi:10.5194/acp-2018-612, 2019  
 1017  
 1018 Dada, L., Paasonen, P., Nieminen, T., Buenrostro Mazon, S., Kontkanen, J., Peräkylä, O.,  
 1019 Lehtipalo, K., Hussein, T., Petäjä, T., Kerminen, V. M., Bäck, J. and Kulmala, M.: Long-term  
 1020 analysis of clear-sky new particle formation events and nonevents in Hyytiälä, *Atmos. Chem. Phys.*,  
 1021 17(10), 6227–6241, doi:10.5194/acp-17-6227-2017, 2017.  
 1022  
 1023 Dai, L., Wang, H., Zhou, L., An, J., Tang, L., Lu, C., Yan, W., Liu, R., Kong, S., Chen, M., Lee, S.  
 1024 and Yu, H.: Regional and local new particle formation events observed in the Yangtze River Delta  
 1025 region, China, *J. Geophys. Res.*, 122(4), 2389–2402, doi:10.1002/2016JD026030, 2017.  
 1026  
 1027 Dal Maso, M., Kulmala, M., Riipinen, I., Wagner, R., Hussein, T., Aalto, P. P. and Lehtinen, K. E.  
 1028 J.: Formation and growth of fresh atmospheric aerosols: Eight years of aerosol size distribution data  
 1029 from SMEAR II, Hyytiälä, Finland, *Boreal Environ. Res.*, 10(5), 323–336,  
 1030 doi:10.1016/j.ijpharm.2012.03.044, 2005.  
 1031  
 1032 Dall’Osto, M., Beddows, D. C. S., Asmi, A., Poulain, L., Hao, L., Freney, E., Allan, J. D.,  
 1033 Canagaratna, M., Crippa, M., Bianchi, F., De Leeuw, G., Eriksson, A., Swietlicki, E., Hansson, H.  
 1034 C., Henzing, J. S., Granier, C., Zemankova, K., Laj, P., Onasch, T., Prevot, A., Putaud, J. P., Sellegri,  
 1035 K., Vidal, M., Virtanen, A., Simo, R., Worsnop, D., O’Dowd, C., Kulmala, M. and Harrison, R. M.:  
 1036 Novel insights on new particle formation derived from a pan-european observing system, *Sci. Rep.*,  
 1037 8(1), 1–11, doi:10.1038/s41598-017-17343-9, 2018.  
 1038  
 1039 Dall’Osto, M., Querol, X., Alastuey, A., O’Dowd, C., Harrison, R. M., Wenger, J. and Gómez-  
 1040 Moreno, F. J.: On the spatial distribution and evolution of ultrafine particles in Barcelona, *Atmos.*  
 1041 *Chem. Phys.*, 13(2), 741–759, doi:10.5194/acp-13-741-2013, 2013.  
 1042  
 1043 Dall’Osto, M., Beddows, D. C. S., Pey, J., Rodriguez, S., Alastuey, A., M. Harrison, R. and Querol,  
 1044 X.: Urban aerosol size distributions over the Mediterranean city of Barcelona, NE Spain, *Atmos.*  
 1045 *Chem. Phys.*, 12(22), 10693–10707, doi:10.5194/acp-12-10693-2012, 2012.  
 1046

1047 Ehn, M., Thornton, J. A., Kleist, E., Sipilä, M., Junninen, H., Pullinen, I., Springer, M., Rubach, F.,  
 1048 Tillmann, R., Lee, B., Lopez-Hilfiker, F., Andres, S., Acir, I. H., Rissanen, M., Jokinen, T.,  
 1049 Schobesberger, S., Kangasluoma, J., Kontkanen, J., Nieminen, T., Kurtén, T., Nielsen, L. B.,  
 1050 Jørgensen, S., Kjaergaard, H. G., Canagaratna, M., Maso, M. D., Berndt, T., Petäjä, T., Wahner, A.,  
 1051 Kerminen, V. M., Kulmala, M., Worsnop, D. R., Wildt, J. and Mentel, T. F.: A large source of low-  
 1052 volatility secondary organic aerosol, *Nature*, 506(7489), 476–479, doi:10.1038/nature13032, 2014.  
 1053  
 1054 Fenske, J. D., Hasson, A.S., Paulson, S. E., Kuwata, K. T., Ho, A., Houk, K. N.: The Pressure  
 1055 Dependence of the OH Radical Yield from Ozone Alkene Reactions *J Phys Chem A*, 104 7821, 2000  
 1056  
 1057 Fuchs, N. A. and Sutugin, A. G.: Highly dispersed aerosols, *Top. Curr. Aerosol Res.*, 1,  
 1058 doi:<https://doi.org/10.1016/B978-0-08-016674-2.50006-6>, 1971.  
 1059  
 1060 Glasoe, W. a, Volz, K., Panta, B., Freshour, N., Bachman, R., Hanson, D. R., Mcmurry, P. H. and  
 1061 Jen, C.: Sulfuric acid nucleation: An experimental study of the effect of seven bases, , 1933–1950,  
 1062 doi:10.1002/2014JD022730, 2015.  
 1063  
 1064 Größ, J., Hamed, A., Sonntag, A., Spindler, G., Manninen, H. E., Nieminen, T., Kulmala, M.,  
 1065 Hõrrak, U., Plass-Dülmer, C., Wiedensohler, A., and Birmili, W.: Atmospheric new particle  
 1066 formation at the research station Melpitz, Germany: connection with gaseous precursors and  
 1067 meteorological parameters, *Atmos. Chem. Phys.*, 18, 1835–1861, [https://doi.org/10.5194/acp-18-](https://doi.org/10.5194/acp-18-1835-2018)  
 1068 1835-2018, 2018.  
 1069  
 1070 Guo, S., Hu, M., Peng, J., Wu, Z., Zamora, M. L., Shang, D., Du, Z., Zheng, J., Fang, X., Tang, R.,  
 1071 Wu, Y., Zeng, L., Shuai, S., Zhang, W., Wang, Y., Ji, Y., Li, Y., Zhang, A. L., Wang, W., Zhang, F.,  
 1072 Zhao, J., Gong, X., Wang, C., Molina, M. J. and Zhang, R.: Remarkable nucleation and growth of  
 1073 ultrafine particles from vehicular exhaust, *Proc. Nat. Acad. Sci. U. S. A.*, 117(7), 3427–3432,  
 1074 doi:10.1073/pnas.1916366117, 2020.  
 1075  
 1076 Hallar, A. G., Petersen, R., McCubbin, I. B., Lowenthal, D., Lee, S., Andrews, E. and Yu, F.:  
 1077 Climatology of new particle formation and corresponding precursors at storm peak laboratory,  
 1078 *Aerosol Air Qual. Res.*, 16(3), 816–826, doi:10.4209/aaqr.2015.05.0341, 2016.  
 1079  
 1080 Hamed, A., Korhonen, H., Sihto, S. L., Joutsensaari, J., Jrvinen, H., Petäjä, T., Arnold, F.,  
 1081 Nieminen, T., Kulmala, M., Smith, J. N., Lehtinen, K. E. J. and Laaksonen, A.: The role of relative  
 1082 humidity in continental new particle formation, *J. Geophys. Res. Atmos.*, 116(3), 1–12,  
 1083 doi:10.1029/2010JD014186, 2011.  
 1084  
 1085 Harrison, R. M.: Urban atmospheric chemistry: A very special case for study, *npj Clim. Atmos. Sci.*,  
 1086 1(1), 5, doi:10.1038/s41612-017-0010-8, 2017.

1087  
1088 Henschel, H., Kurtén, T., Vehkamäki, H.: Computational study on the effect of hydration on new  
1089 particle formation in the sulfuric acid/ammonia and sulfuric acid/dimethylamine systems, *J. Phys.*  
1090 *Chem. A* 2016, 120, 11, 1886–1896, 2016.  
1091  
1092  
1093 Hidy, G. M.: Atmospheric sulfur and nitrogen oxides, Academic Press, ISBN: 9781483288666,  
1094 1994  
1095  
1096 Hietikko, R., Kuuluvainen, H., Harrison, R. M., Portin, H., Timonen, H., Niemi, J. V and Rönkkö,  
1097 T.: Diurnal variation of nanocluster aerosol concentrations and emission factors in a street canyon,  
1098 *Atmos. Environ.*, 189, 98–106, doi:10.1016/j.atmosenv.2018.06.031, 2018.  
1099  
1100 Iida, K., Stolzenburg, M. R., McMurry, P. H. and Smith, J. N.: Estimating nanoparticle growth rates  
1101 from size-dependent charged fractions: Analysis of new particle formation events in Mexico City, *J.*  
1102 *Geophys. Res. Atmos.*, 113(5), 1–15, doi:10.1029/2007JD009260, 2008.  
1103  
1104 Järvi, L., Hannuniemi, H., Hussein, T., Junninen, H., Aalto, P., Hillamo, R., Mäkelä, T., Keronen, P.  
1105 and Siivola, E.: The urban measurement station SMEAR III : Continuous monitoring of air pollution  
1106 and surface – atmosphere interactions in Helsinki , Finland, 14(April), 86–109, 2009.  
1107  
1108 Jayaratne, R., Pushpawela, B., He, C., Li, H., Gao, J., Chai, F. and Morawska, L.: Observations of  
1109 particles at their formation sizes in Beijing, China, *Atmos. Chem. Phys.*, 17(14), 8825–8835,  
1110 doi:10.5194/acp-17-8825-2017, 2017.  
1111  
1112 Jeong, C.-H. H., Evans, G. J., McGuire, M. L., Y.-W. Chang, R., Abbatt, J. P. D. D., Zeromskiene,  
1113 K., Mozurkewich, M., Li, S.-M. M., Leaitch, W. R., Chang, R. Y.-W., Abbatt, J. P. D. D.,  
1114 Zeromskiene, K., Mozurkewich, M., Li, S.-M. M. and Leaitch, W. R.: Particle formation and growth  
1115 at five rural and urban sites, *Atmos. Chem. Phys.*, 10(16), 7979–7995, doi:10.5194/acp-10-7979-  
1116 2010, 2010.  
1117  
1118 [Jung, J., Adams P. J., and Pandis, S. N., Simulating the size distribution and chemical composition](#)  
1119 [of ultrafine particles during nucleation events, \*Atmos. Environ.\*, 40, 2248–2259,](#)  
1120 [doi:10.1016/j.atmosenv.2005.09.082, 2006.](#)  
1121  
1122 [Jung, J. G., Pandis, S. N., and Adams, P. J., Evaluation of nucleation theories in a sulfur-rich](#)  
1123 [environment, \*Aerosol Sci. Technol.\*, 42, 495–504, doi:10.1080/02786820802187085, 2008.](#)  
1124  
1125 [Kalivitis, N., Kerminen, V.-M., Kouvarakis, G., Stavroulas, I., Tzitzikalaki, E., Kalkavouras, P.,](#)  
1126 [Daskalakis, N., Myriokefalitakis, S., Bougatioti, A., Manninen, H. E., Roldin, P., Petäjä, T., Boy,](#)

1127 [M., Kulmala, M., Kanakidou, M. and Mihalopoulos N.: Formation and growth of atmospheric](#)  
 1128 [nanoparticles in the eastern Mediterranean: Results from long-term measurements and process](#)  
 1129 [simulations', Atmospheric Chemistry and Physics Discussions, pp. 1–38. doi: 10.5194/acp-2018-](#)  
 1130 [229, 2019.](#)  
 1131

1132 Kalkavouras, P., Bossioli, E., Bezantakos, S., Bougiatioti, A., Kalivitis, N., Stavroulas, I.,  
 1133 Kouvarakis, G., Protonotariou, A. P., Dandou, A., Biskos, G., Mihalopoulos, N., Nenes, A. and  
 1134 Tombrou, M.: New particle formation in the southern Aegean Sea during the Etesians: Importance  
 1135 for CCN production and cloud droplet number, *Atmos. Chem. Phys.*, 17(1), 175–192,  
 1136 doi:10.5194/acp-17-175-2017, 2017.  
 1137

1138 Kerminen, V., Lehtinen, K. E. J., Anttila, T., Kulmala, M., Lehtinen, K. E. J., Anttila, T. and Kulmala,  
 1139 M.: Dynamics of atmospheric nucleation mode particles : a timescale analysis, *Tellus*, 56B, 135–146,  
 1140 doi:10.3402/tellusb.v56i2.16411, 2004.  
 1141

1142 Kerminen, V. M., Pirjola, L. and Kulmala, M.: How significantly does coagulation scavenging limit  
 1143 atmospheric particle production?, *J. Geophys. Res. Atmos.*, 106(D20), 24119–24125,  
 1144 doi:10.1029/2001JD000322, 2001.  
 1145

1146 Kerminen, V. M., Kulmala, M., Worsnop, D. R., Wildt, J. and Mentel, T. F.: A large source of low-  
 1147 volatility secondary organic aerosol, *Nature*, 506(7489), 476–479, doi:10.1038/nature13032, 2014.  
 1148

1149 Ketzel, M., Wåhlin, P., Kristensson, A., Swietlicki, E., Berkowicz, R., Nielsen, O. J. and Palmgren,  
 1150 F.: Particle size distribution and particle mass measurements at urban, near-city and rural level in the  
 1151 Copenhagen area and Southern Sweden, *Atmos. Chem. Phys. Discuss.*, 3(6), 5513–5546,  
 1152 doi:10.5194/acpd-3-5513-2003, 2004.  
 1153

1154 Kiendler-Scharr, A., Wildt, J., Dal Maso, M., Hohaus, T., Kleist, E., Mentel, T. F., Tillmann, R.,  
 1155 Uerlings, R., Schurr, U. and Wahner, A.: New particle formation in forests inhibited by isoprene  
 1156 emissions, 461, 381–384, 2009.  
 1157

1158 Kim, K. H., Kabir, E. and Kabir, S.: A review on the human health impact of airborne particulate  
 1159 matter, *Environ. Int.*, 74, 136–143, doi:10.1016/j.envint.2014.10.005, 2015.  
 1160

1161 Kirkby, J., Curtius, J., Almeida, J., Dunne, E., Duplissy, J., Ehrhart, S., Franchin, A., Gagné, S., Ickes,  
 1162 L., Kürten, A., Kupc, A., Metzger, A., Riccobono, F., Rondo, L., Schobesberger, S., Tsagkogeorgas,  
 1163 G., Wimmer, D., Amorim, A., Bianchi, F., Breitenlechner, M., David, A., Dommen, J., Downard, A.,  
 1164 Ehn, M., Flagan, R. C., Haider, S., Hansel, A., Hauser, D., Jud, W., Junninen, H., Kreissl, F., Kvashin,  
 1165 A., Laaksonen, A., Lehtipalo, K., Lima, J., Lovejoy, E. R., Makhmutov, V., Mathot, S., Mikkilä, J.,  
 1166 Minginette, P., Mogo, S., Nieminen, T., Onnela, A., Pereira, P., Petäjä, T., Schnitzhofer, R., Seinfeld,

1167 J. H., Sipilä, M., Stozhkov, Y., Stratmann, F., Tomé, A., Vanhanen, J., Viisanen, Y., Vrtala, A.,  
 1168 Wagner, P. E., Walther, H., Weingartner, E., Wex, H., Winkler, P. M., Carslaw, K. S., Worsnop, D.  
 1169 R., Baltensperger, U. and Kulmala, M.: Role of sulphuric acid, ammonia and galactic cosmic rays in  
 1170 atmospheric aerosol nucleation, *Nature*, 476(7361), 429–435, doi:10.1038/nature10343, 2011.  
 1171  
 1172 Korhonen, P., Kulmala, M., Laaksonen, A., Viisanen, Y., Mcgraw, R. and Seinfeld, J. H.: Ternary  
 1173 nucleation of H<sub>2</sub>SO<sub>4</sub>, NH<sub>3</sub> and H<sub>2</sub>O in the atmosphere, *J. Geophys. Res.*, 104(D21), 26349–26353,  
 1174 1999.  
 1175  
 1176 Kulmala, M., Petäjä, T., Mönkkönen, P., Koponen, I. K., Dal Maso, M., Aalto, P. P., Lehtinen, K.  
 1177 E. J. and Kerminen, V.-M.: On the growth of nucleation mode particles: source rates of condensable  
 1178 vapor in polluted and clean environments, *Atmos. Chem. Phys. Discuss.*, 4(5), 6943–6966,  
 1179 doi:10.5194/acpd-4-6943-2004, 2005.  
 1180  
 1181 Kulmala, M. and Kerminen, V. M.: On the formation and growth of atmospheric nanoparticles,  
 1182 *Atmos. Res.*, 90(2–4), 132–150, doi:10.1016/j.atmosres.2008.01.005, 2008.  
 1183  
 1184 Kulmala, M., Kerminen, V.-M. M., Petäjä, T., Ding, A. J. and Wang, L.: Atmospheric gas-to-particle  
 1185 conversion: Why NPF events are observed in megacities?, *Faraday Discuss.*, 200, 271–288,  
 1186 doi:10.1039/c6fd00257a, 2017.  
 1187  
 1188 Kulmala, M., Petäjä, T., Nieminen, T., Sipilä, M., Manninen, H. E., Lehtipalo, K., Dal Maso, M.,  
 1189 Aalto, P. P., Junninen, H., Paasonen, P., Riipinen, I., Lehtinen, K. E. J., Laaksonen, A. and Kerminen,  
 1190 V. M.: Measurement of the nucleation of atmospheric aerosol particles, *Nat. Protoc.*, 7(9), 1651–  
 1191 1667, doi:10.1038/nprot.2012.091, 2012.  
 1192  
 1193 Kulmala, M., Petäjä, T., Mönkkönen, P., Koponen, I. K., Dal Maso, M., Aalto, P. P., Lehtinen, K. E.  
 1194 J. and Kerminen, V.-M.: On the growth of nucleation mode particles: source rates of condensable  
 1195 vapor in polluted and clean environments, *Atmos. Chem. Phys. Discuss.*, 4(5), 6943–6966,  
 1196 doi:10.5194/acpd-4-6943-2004, 2005.  
 1197  
 1198 Kulmala, M., Dal Maso, M., Mäkelä, J. M., Pirjola, L., Väkevä, M., Aalto, P., Miikkulainen, P.,  
 1199 Hämeri, K. and O’Dowd, C. D.: On the formation, growth and composition of nucleation mode  
 1200 particles, *Tellus, Ser. B Chem. Phys. Meteorol.*, 53(4), 479–490, doi:10.3402/tellusb.v53i4.16622,  
 1201 2001.  
 1202  
 1203 Kürten, A., Li, C., Bianchi, F., Curtius, J., Dias, A., Donahue, N. M., Duplissy, J., Flagan, R. C.,  
 1204 Hakala, J., Jokinen, T., Kirkby, J., Kulmala, M., Laaksonen, A., Lehtipalo, K., Makhmutov, V.,  
 1205 Onnela, A., Rissanen, M. P., Simon, M., Sipilä, M., Stozhkov, Y., Tröstl, J., Ye, P., and McMurry, P.  
 1206 H.: New particle formation in the sulfuric acid–dimethylamine–water system: reevaluation of

1207 CLOUD chamber measurements and comparison to an aerosol nucleation and growth model, *Atmos.*  
1208 *Chem. Phys.*, 18, 845–863, <https://doi.org/10.5194/acp-18-845-2018>, 2018.

1209

1210 Kürten, A., Bergen, A., Heinritzi, M., Leiminger, M., Lorenz, V., Piel, F., Simon, M., Sitals, R.,  
1211 Wagner, A. C. and Curtius, J.: Observation of new particle formation and measurement of sulfuric  
1212 acid, ammonia, amines and highly oxidized organic molecules at a rural site in central Germany,  
1213 *Atmos. Chem. Phys.*, 16(19), 12793–12813, doi:10.5194/acp-16-12793-2016, 2016.

1214

1215 Lee, S.-H. H., Uin, J., Guenther, A. B., de Gouw, J. A., Yu, F., Nadykto, A. B., Herb, J., Ng, N. L.,  
1216 Koss, A., Brune, W. H., Baumann, K., Kanawade, V. P., Keutsch, F. N., Nenes, A., Olsen, K.,  
1217 Goldstein, A. and Ouyang, Q.: Isoprene suppression of new particle formation: Potential  
1218 mechanisms and implications, *J. Geophys. Res. Atmos.*, 121(24), 14,621–14,635,  
1219 doi:10.1002/2016JD024844, 2016.

1220

1221 Lehtinen, K. E. J., Korhonen, H., Dal Maso, M. and Kulmala, M.: On the concept of condensation  
1222 sink diameter, *Boreal Environ. Res.*, 8(4), 405–411, 2003.

1223

1224 Lehtipalo, K., Yan, C., Dada, L., Bianchi, F., Xiao, M., Wagner, R., Stolzenburg, D., Ahonen, L. R.,  
1225 Amorim, A., Baccarini, A., Bauer, P. S., Baumgartner, B., Bergen, A., Bernhammer, A.,  
1226 Breitenlechner, M., Brilke, S., Buchholz, A., Mazon, S. B., Chen, D., Chen, X., Dias, A., Dommen,  
1227 J., Draper, D. C., Duplissy, J., Ehn, M., Finkenzeller, H., Fischer, L., Frege, C., Fuchs, C., Garmash,  
1228 O., Gordon, H., Hakala, J., He, X., Heikkinen, L., Heinritzi, M., Helm, J. C., Hofbauer, V., Hoyle, C.  
1229 R., Jokinen, T., Ojdanic, A., Onnela, A., Passananti, M., Petäjä, T., Piel, F., Sarnela, N., Schallhart,  
1230 S., Schuchmann, S., Sengupta, K. and Simon, M.: Multicomponent new particle formation from  
1231 sulfuric acid, ammonia, and biogenic vapors, (3), 1–10, 2018.

1232

1233 Li, X., Chee, S., Hao, J., Abbatt, J. P. D., Jiang, J. and Smith, J. N.: Relative humidity effect on the  
1234 formation of highly oxidized molecules and new particles during monoterpene oxidation, *Atmos.*  
1235 *Chem. Phys.*, 19(3), 1555–1570, doi:10.5194/acp-19-1555-2019, 2019.

1236

1237 Makkonen, R., Asmi, A., Kerminen, V. M., Boy, M., Arneth, A., Hari, P. and Kulmala, M.: Air  
1238 pollution control and decreasing new particle formation lead to strong climate warming, *Atmos.*  
1239 *Chem. Phys.*, 12(3), 1515–1524, doi:10.5194/acp-12-1515-2012, 2012.

1240

1241 McFiggans, G., Mentel, T. F., Wildt, J., Pullinen, I., Kang, S., Kleist, E., Schmitt, S., Springer, M.,  
1242 Tillmann, R., Wu, C., Zhao, D., Hallquist, M., Faxon, C., Le Breton, M., Hallquist, Å. M., Simpson,  
1243 D., Bergström, R., Jenkin, M. E., Ehn, M., Thornton, J. A., Alfarra, M. R., Bannan, T. J., Percival, C.  
1244 J., Priestley, M., Topping, D. and Kiendler-Scharr, A.: Secondary organic aerosol reduced by mixture  
1245 of atmospheric vapours, *Nature*, 565(7741), 587–593, doi:10.1038/s41586-018-0871-y, 2019.

1246 Merikanto, J., Spracklen, D. V., Mann, G. W., Pickering, S. J. and Carslaw, K. S.: Impact of



1247 nucleation on global CCN, *Atmos. Chem. Phys.*, 9(21), 8601–8616, doi:10.5194/acp-9-8601-2009,  
1248 2009.

1249

1250 Merikanto, J., Spracklen, D. V., Mann, G. W., Pickering, S. J. and Carslaw, K. S.: Impact of  
1251 nucleation on global CCN, *Atmos. Chem. Phys.*, 9(21), 8601–8616, doi:10.5194/acp-9-8601-2009,  
1252 2009.

1253

1254 Metzger, A., Verheggen, B., Dommen, J., Duplissy, J., Prevot, A. S. H., Weingartner, E., Riipinen,  
1255 I., Kulmala, M., Spracklen, D. V., Carslaw, K. S. and Baltensperger, U.: Evidence for the role of  
1256 organics in aerosol particle formation under atmospheric conditions, *Proc. Nat. Acad. Sci.*, 107(15),  
1257 6646–6651, doi:10.1073/pnas.0911330107, 2010.

1258

1259 Minguillón, M. C., Brines, M., Pérez, N., Reche, C., Pandolfi, M., Fonseca, A. S., Amato, F.,  
1260 Alastuey, A., Lyasota, A., Codina, B., Lee, H. K., Eun, H. R., Ahn, K. H. and Querol, X.: New particle  
1261 formation at ground level and in the vertical column over the Barcelona area, *Atmos. Res.*, 164–165,  
1262 118–130, doi:10.1016/j.atmosres.2015.05.003, 2015.

1263

1264 Mirabel, P. and Katz, J. L.: Binary homogeneous nucleation as a mechanism for the formation of  
1265 aerosols, *J. Chem. Phys.*, 60(3), 1138–1144, doi:10.1063/1.1681124, 1974.

1266

1267 Mølgaard, B., Birmili, W., Clifford, S., Massling, A., Eleftheriadis, K., Norman, M., Vratolis, S.,  
1268 Wehner, B., Corander, J., Hämeri, K. and Hussein, T.: Evaluation of a statistical forecast model for  
1269 size-fractionated urban particle number concentrations using data from five European cities, *J.*  
1270 *Aerosol Sci.*, 66, 96–110, doi:10.1016/j.jaerosci.2013.08.012, 2013.

1271

1272 Molteni, U., Bianchi, F., Klein, F., El Haddad, I., Frege, C., Rossi, M. J., Dommen, J. and  
1273 Baltensperger, U.: Formation of highly oxygenated organic molecules from aromatic compounds,  
1274 *Atmos. Chem. Phys.*, 18(3), 1909–1921, doi:10.5194/acp-18-1909-2018, 2018.

1275

1276 Napari, I., Noppel, M., Vehkamäki, H. and Kulmala, M.: An improved model for ternary nucleation  
1277 of sulfuric acid-ammonia-water, *J. Chem. Phys.*, 116(10), 4221–4227, doi:10.1063/1.1450557, 2002.

1278

1279 Nieminen, T., Kerminen, V.-M., Petäjä, T., Aalto, P. P., Arshinov, M., Asmi, E., Baltensperger, U.,  
1280 Beddows, D. C. S., Beukes, J. P., Collins, D., Ding, A., Harrison, R. M., Henzing, B., Hooda, R., Hu,  
1281 M., Hörrak, U., Kivekäs, N., Komsaare, K., Krejci, R., Kristensson, A., Laakso, L., Laaksonen, A.,  
1282 Leaitch, W. R., Lihavainen, H., Mihalopoulos, N., Németh, Z., Nie, W., O ’dowd, C., Salma, I.,  
1283 Sellegri, K., Svenningsson, B., Swietlicki, E., Tunved, P., Ulevicius, V., Vakkari, V., Vana, M.,  
1284 Wiedensohler, A., Wu, Z., Virtanen, A., Kulmala, M., O ’dowd, C., Salma, I., Sellegri, K., Svenningsson,  
1285 B., Swietlicki, E., Tunved, P., Ulevicius, V., Vakkari, V., Vana, M., Wiedensohler,  
1286 A., Wu, Z., Virtanen, A., Kulmala, M., O ’dowd, C., Salma, I., Sellegri, K., Svenningsson, B.,

1287 Swietlicki, E., Tunved, P., Ulevicius, V., Vakkari, V., Vana, M., Wiedensohler, A., Wu, Z., Virtanen,  
 1288 A. and Kulmala, M.: Global analysis of continental boundary layer new particle formation based on  
 1289 long-term measurements, *Atmos. Chem. Phys. Discuss.*, 5194, 2018–304, doi:10.5194/acp-2018-304,  
 1290 2018.  
 1291  
 1292 Nieminen, T., Lehtinen, K. E. J. and Kulmala, M.: Sub-10 nm particle growth by vapor condensation-  
 1293 effects of vapor molecule size and particle thermal speed, *Atmos. Chem. Phys.*, 10(20), 9773–9779,  
 1294 doi:10.5194/acp-10-9773-2010, 2010.  
 1295  
 1296 O’Dowd, C. D., Jimenez, J. L., Bahreini, R., Flagan, R. C., Seinfeld, J. H., Hameri Kaarle, Pirjola,  
 1297 L., Kulmala, M., Jennings, S. G. and Hoffmann, T.: Marine aerosol formation from biogenic iodine  
 1298 emissions, *Lett. to Nat.*, 417(June), 1–5, doi:10.1038/nature00773.1.2.3.4.5.6.7.8.9.10., 2002.  
 1299  
 1300 Olenius, T., Halonen, R., Kurten, T., Henschel, H., Maatta, O. K., Ortega, I. K., Jen, C.,  
 1301 Vehkamäki, H. and Riipinen, I.: New particle formation from sulfuric acid amines: Comparison of  
 1302 monomethylamine, dimethylamine, and trimethylamine, *J. Geophys. Res. Atmos.*, 7103–7118,  
 1303 doi:10.1002/2017JD026501, 2017.  
 1304  
 1305 Olin, M., Kuuluvainen, H., Aurela, M., Kalliokoski, J., Kuittinen, N., Isotalo, M., Timonen, H. J.,  
 1306 Niemi, J. V., Rönkkö, T., and Dal Maso, M.: Traffic-originated nanocluster emission exceeds  
 1307 H<sub>2</sub>SO<sub>4</sub>-driven photochemical new particle formation in an urban area, *Atmos. Chem. Phys.*, 20, 1–  
 1308 13, <https://doi.org/10.5194/acp-20-1-2020>, 2020.  
 1309  
 1310 Paasonen, P., Asmi, A., Petäjä, T., Kajos, M. K., Äijälä, M., Junninen, H., Holst, T., Abbatt, J. P.  
 1311 D., Arneth, A., Birmili, W., Van Der Gon, H. D., Hamed, A., Hoffer, A., Laakso, L., Laaksonen,  
 1312 A., Richard Leaitch, W., Plass-Dülmer, C., Pryor, S. C., Räisänen, P., Swietlicki, E., Wiedensohler,  
 1313 A., Worsnop, D. R., Kerminen, V. M. and Kulmala, M.: Warming-induced increase in aerosol  
 1314 number concentration likely to moderate climate change, *Nat. Geosci.*, 6(6), 438–442,  
 1315 doi:10.1038/ngeo1800, 2013.  
 1316  
 1317 Park, M., Yum, S. S. and Kim, J. H.: Characteristics of submicron aerosol number size distribution  
 1318 and new particle formation events measured in Seoul, Korea, during 2004–2012, *Asia-Pacific J.*  
 1319 *Atmos. Sci.*, 51(1), 1–10, doi:10.1007/s13143-014-0055-0, 2015.  
 1320  
 1321 Petäjä, T., Mauldin, R. L., Kosciuch, E., McGrath, J., Nieminen, T., Paasonen, P., Boy, M.,  
 1322 Adamov, A., Kotiaho, T. and Kulmala, M.: Sulfuric acid and OH concentrations in a boreal forest  
 1323 site, *Atmos. Chem. Phys.*, 9(19), 7435–7448, doi:10.5194/acp-9-7435-2009, 2009.  
 1324  
 1325 Pikridas, M., Sciare, J., Freutel, F., Crumeyrolle, S., Von Der Weiden-Reinmüller, S. L., Borbon, A.,  
 1326 Schwarzenboeck, A., Merkel, M., Crippa, M., Kostenidou, E., Psichoudaki, M., Hildebrandt, L.,

1327 Engelhart, G. J., Petäjä, T., Prévôt, A. S. H., Drewnick, F., Baltensperger, U., Wiedensohler, A.,  
 1328 Kulmala, M., Beekmann, M. and Pandis, S. N.: In situ formation and spatial variability of particle  
 1329 number concentration in a European megacity, *Atmos. Chem. Phys.*, 15(17), 10219–10237,  
 1330 doi:10.5194/acp-15-10219-2015, 2015.  
 1331  
 1332 Pillai, P., Khlystov, A., Walker, J. and Aneja, V.: Observation and analysis of particle nucleation at  
 1333 a forest site in southeastern US, *Atmosphere (Basel)*, 4(2), 72–93, doi:10.3390/atmos4020072, 2013.  
 1334  
 1335 Poling, B. E., Prausnitz, J. M. and O’Connell, J. P.: *The properties of gases and liquids*, 5th ed.,  
 1336 McGraw-Hill Education., 2001.  
 1337  
 1338 Politis, M., Pilinis, C. and Lekkas, T. D.: Ultrafine particles (UFP) and health effects. Dangerous.  
 1339 Like no other PM? Review and analysis, *Glob. Nest J.*, 10(3), 439–452, 2008.  
 1340  
 1341 Quéléver, L. L. J., Kristensen, K., Normann Jensen, L., Rosati, B., Teiwes, R., Daellenbach, K. R.,  
 1342 Peräkylä, O., Roldin, P., Bossi, R., Pedersen, H. B., Glasius, M., Bilde, M. and Ehn, M.: Effect of  
 1343 temperature on the formation of highly oxygenated organic molecules (HOMs) from alpha-pinene  
 1344 ozonolysis, *Atmos. Chem. Phys.*, 19(11), 7609–7625, doi:10.5194/acp-19-7609-2019, 2019.  
 1345  
 1346 Querol, X., Gangoiti, G., Mantilla, E., Alastuey, A., Minguillón, M. C., Amato, F., Reche, C., Viana,  
 1347 M., Moreno, T., Karanasiou, A., Rivas, I., Pérez, N., Ripoll, A., Brines, M., Ealo, M., Pandolfi, M.,  
 1348 Lee, H. K., Eun, H. R., Park, Y. H., Escudero, M., Beddows, D., Harrison, R. M., Bertrand, A.,  
 1349 Marchand, N., Lysota, A., Codina, B., Olid, M., Udina, M., Jiménez-Esteve, B. B., Jiménez-Esteve,  
 1350 B. B., Alonso, L., Millán, M. and Ahn, K. H.: Phenomenology of high-ozone episodes in NE Spain,  
 1351 *Atmos. Chem. Phys.*, 17(4), 2817–2838, doi:10.5194/acp-17-2817-2017, 2017.  
 1352  
 1353 Riccobono, F., Schobesberger, S., Scott, C. E., Dommen, J., Ortega, I. K., Rondo, L., Almeida, J.,  
 1354 Amorim, A., Bianchi, F., Breitenlechner, M., David, A., Downard, A., Dunne, E. M., Duplissy, J.,  
 1355 Ehrhart, S., Flagan, R. C., Franchin, A., Hansel, A., Junninen, H., Kajos, M., Keskinen, H., Kupc, A.,  
 1356 Makhmutov, V., Mathot, S., Nieminen, T., Onnela, A., Petäjä, T., Tsagkogeorgas, G., Vaattovaara,  
 1357 P., Viisanen, Y., Vrtala, A. and Wagner, P. E.: Oxidation Products of biogenic atmospheric particles,  
 1358 *Science*, 717, 717–722, doi:10.1126/science.1243527, 2014.  
 1359  
 1360 Rimnácová, D., Ždímal, V., Schwarz, J., Smolík, J. and Rimnác, M.: Atmospheric aerosols in suburb  
 1361 of Prague: The dynamics of particle size distributions, *Atmos. Res.*, 101(3), 539–552,  
 1362 doi:10.1016/j.atmosres.2010.10.024, 2011.  
 1363 Rose, C., Zha, Q., Dada, L., Yan, C., Lehtipalo, K., Junninen, H., Mazon, S. B., Jokinen, T., Sarnela,  
 1364 N., Sipilä, M., Petäjä, T., Kerminen, V. M., Bianchi, F. and Kulmala, M.: Observations of biogenic  
 1365 ion-induced cluster formation in the atmosphere, *Sci. Adv.*, 4(4), 1–10, doi:10.1126/sciadv.aar5218,  
 1366 2018.

1367  
1368 Rivas, I., Beddows, D. C. S., Amato, F., Green, D. C., Järvi, L., Hueglin, C., Reche, C., Timonen, H.,  
1369 Fuller, G. W., Niemi, J. V, Pérez, N., Aurela, M., Hopke, P. K., Alastuey, A., Kulmala, M., Harrison,  
1370 R. M., Querol, X. and Kelly, F. J.: Source apportionment of particle number size distribution in urban  
1371 background and traffic stations in four European cities, *Environ. Int.*, 135, 105345,  
1372 doi:10.1016/j.envint.2019.105345, 2020.  
1373  
1374 Rizzo, L. V., Artaxo, P., Karl, T., Guenther, A. B. and Greenberg, J.: Aerosol properties, in-canopy  
1375 gradients, turbulent fluxes and VOC concentrations at a pristine forest site in Amazonia, *Atmos.*  
1376 *Environ.*, 44(4), 503–511, doi:10.1016/j.atmosenv.2009.11.002, 2010.  
1377  
1378 Salma, I., Borsòs, T., Weidinger, T., Aalto, P., Hussein, T., Dal Maso, M. and Kulmala, M.:  
1379 Production, growth and properties of ultrafine atmospheric aerosol particles in an urban environment,  
1380 *Atmos. Chem. Phys.*, 11(3), 1339–1353, doi:10.5194/acp-11-1339-2011, 2011.  
1381  
1382 Schwartz, J., Dockery, D. W. and Neas, L. M.: Is Daily Mortality Associated Specifically with Fine  
1383 Particles?, *J. Air Waste Manag. Assoc.*, 46(10), 927–939, doi:10.1080/10473289.1996.10467528,  
1384 1996.  
1385  
1386 Seinfeld, J. H. and Pandis, S. N.: *Atmospheric Chemistry and Physics: From Air Pollution to Climate*  
1387 *Change*, 3rd Editio., John Wiley & Sons, Inc, New Jersey, Canada, 2012.  
1388  
1389 Shen, X., Sun, J., Kivekäs, N., Kristensson, A., Zhang, X., Zhang, Y., Zhang, L., Fan, R., Qi, X., Ma,  
1390 Q. and Zhou, H.: Spatial distribution and occurrence probability of regional new particle formation  
1391 events in eastern China, *Atmos. Chem. Phys.*, 18(2), 587–599, doi:10.5194/acp-18-587-2018, 2018.  
1392  
1393 Shrivastava, M., Cappa, C. D., Fan, J., Goldstein, A. H., Guenther, A. B., Jimenez, J. L., Kuang, C.,  
1394 Laskin, A., Martin, S. T., Ng, N. L., Petaja, T., Pierce, J. R., Rasch, P. J., Roldin, P., Seinfeld, J. H.,  
1395 Shilling, J., Smith, J. N., Thornton, J. A., Volkamer, R., Wang, J., Worsnop, D. R., Zaveri, R. A.,  
1396 Zelenyuk, A. and Zhang, Q.: Recent advances in understanding secondary organic aerosol:  
1397 Implications for global climate forcing, *Rev. Geophys.*, 55(2), 509–559,  
1398 doi:10.1002/2016RG000540, 2017.  
1399  
1400 Siakavaras, D., Samara, C., Petrakakis, M. and Biskos, G.: Nucleation events at a coastal city during  
1401 the warm period: Kerbside versus urban background measurements, *Atmos. Environ.*, 140, 60–68,  
1402 doi:10.1016/j.atmosenv.2016.05.054, 2016.  
1403  
1404 Sipila, M., Berndt, T., Petaja, T., Brus, D., Vanhanen, J., Stratmann, F., Patokoski, J., Mauldin III,  
1405 R. L., Hyvarinen, A. P., Lihavainen, H. and Kulmala, M.: The Role of Sulfuric Acid in  
1406 Atmospheric Nucleation, *Science*, 327, 1243–1246, doi:10.1126/science.1180315, 2010.

1407

1408 Spracklen, D. V., Carslaw, K. S., Merikanto, J., Mann, G. W., Reddington, C. L., Pickering, S., Ogren,  
1409 J. A., Andrews, E., Baltensperger, U., Weingartner, E., Boy, M., Kulmala, M., Laakso, L.,  
1410 Lihavainen, H., Kivekäs, N., Komppula, M., Mihalopoulos, N., Kouvarakis, G., Jennings, S. G.,  
1411 O'Dowd, C., Birmili, W., Wiedensohler, A., Weller, R., Gras, J., Laj, P., Sellegri, K., Bonn, B.,  
1412 Krejci, R., Laaksonen, A., Hamed, A., Minikin, A., Harrison, R. M., Talbot, R. and Sun, J.: Explaining  
1413 global surface aerosol number concentrations in terms of primary emissions and particle formation,  
1414 *Atmos. Chem. Phys.*, 10(10), 4775–4793, doi:10.5194/acp-10-4775-2010, 2010.

1415

1416 Stolzenburg, D., Simon, M., Ranjithkumar, A., Kürten, A., Lehtipalo, K., Gordon, H., Ehrhart, S.,  
1417 Finkenzeller, H., Pichelstorfer, L., Nieminen, T., He, X.-C., Brilke, S., Xiao, M., Amorim, A.,  
1418 Baalbaki, R., Baccarini, A., Beck, L., Bräkling, S., Caudillo Murillo, L., Chen, D., Chu, B., Dada,  
1419 L., Dias, A., Dommen, J., Duplissy, J., El Haddad, I., Fischer, L., Gonzalez Carracedo, L., Heinritzi,  
1420 M., Kim, C., Koenig, T. K., Kong, W., Lamkaddam, H., Lee, C. P., Leiminger, M., Li, Z.,  
1421 Makhmutov, V., Manninen, H. E., Marie, G., Marten, R., Müller, T., Nie, W., Partoll, E., Petäjä, T.,  
1422 Pfeifer, J., Philippov, M., Rissanen, M. P., Rörup, B., Schobesberger, S., Schuchmann, S., Shen, J.,  
1423 Sipilä, M., Steiner, G., Stozhkov, Y., Tauber, C., Tham, Y. J., Tomé, A., Vazquez-Pufleau, M.,  
1424 Wagner, A. C., Wang, M., Wang, Y., Weber, S. K., Wimmer, D., Wlasits, P. J., Wu, Y., Ye, Q.,  
1425 Zauner-Wieczorek, M., Baltensperger, U., Carslaw, K. S., Curtius, J., Donahue, N. M., Flagan, R.  
1426 C., Hansel, A., Kulmala, M., Lelieveld, J., Volkamer, R., Kirkby, J., and Winkler, P. M.: Enhanced  
1427 growth rate of atmospheric particles from sulfuric acid, *Atmos. Chem. Phys.*, 20, 7359–7372,  
1428 <https://doi.org/10.5194/acp-20-7359-2020>, 2020.

1429

1430 Stolzenburg, D., Fischer, L., Vogel, A. L., Heinritzi, M., Schervish, M. and Simon, M., Wagner, A.  
1431 C., Dada, L., Ahonen, L. R., Amorim, A., Baccarini, A., Bauer, P. S., Baumgartner, B., Bergen, A.,  
1432 Bianchi, F., Breitenlechner, M., Brilke, S., Buenorstro Mazon, S., Chen, D., Dias, A., Draper, D. C.,  
1433 Duplissy, J., El Haddad, I., Finkenzeller, H., Frege, C., Fuchs, C., Garmash, O., Gordon, H., He, X.,  
1434 Helm, J., Hofbauer, V., Hoyle, C. R., Kim, C., Kirkby, J., Kontkanen, J., Kürten, A., Lampilahti, J.,  
1435 Lawler, M., Lehtipalo, K., Leiminger, M., Mai, H., Mathot, S., Mentler, B., Molteni, U., Nie, W.,  
1436 Nieminen, T., Nowak, J. B., Ojdanic, A., Onnela, A., Passananti, M., Petäjä, T., Quéléver, L. L. J.,  
1437 Rissanen, M. P., Sarnela, N., Schallhart, S., Tauber, C., Tome, A., Wagner, R., Wang, M., Weitz,  
1438 L., Wimmer, D., Xiao, M., Yan, C., Ye, P., Zha, Q., Baltensperger, U., Curtius, J., Dommen, J.,  
1439 Flagan, R. C., Kulmala, M., Smith, J. N., Worsnop, D. R., Hansel, A., Donahue, N. M., Winkler, P.  
1440 M.: Rapid growth of organic aerosol nanoparticles over a wide tropospheric temperature range,  
1441 *PNAS* , 115(37), doi:10.1073/pnas.1807604115, 2018.

1442

1443 Tröstl, J., Chuang, W. K., Gordon, H., Heinritzi, M., Yan, C., Molteni, U., Ahlm, L., Frege, C.,  
1444 Bianchi, F., Wagner, R., Simon, M., Lehtipalo, K., Williamson, C., Craven, J. S., Duplissy, J.,  
1445 Adamov, A., Almeida, J., Bernhammer, A. K., Breitenlechner, M., Brilke, S., Dias, A., Ehrhart, S.,  
1446 Flagan, R. C., Franchin, A., Fuchs, C., Guida, R., Gysel, M., Hansel, A., Hoyle, C. R., Jokinen, T.,

1447 Junninen, H., Kangasluoma, J., Keskinen, H., Kim, J., Krapf, M., Kürten, A., Laaksonen, A., Lawler,  
 1448 M., Leiminger, M., Mathot, S., Möhler, O., Nieminen, T., Onnela, A., Petäjä, T., Piel, F. M.,  
 1449 Miettinen, P., Rissanen, M. P., Rondo, L., Sarnela, N., Schobesberger, S., Sengupta, K., Sipilä, M.,  
 1450 Smith, J. N., Steiner, G., Tomè, A., Virtanen, A., Wagner, A. C., Weingartner, E., Wimmer, D.,  
 1451 Winkler, P. M., Ye, P., Carslaw, K. S., Curtius, J., Dommen, J., Kirkby, J., Kulmala, M., Riipinen, I.,  
 1452 Worsnop, D. R., Donahue, N. M. and Baltensperger, U.: The role of low-volatility organic compounds  
 1453 in initial particle growth in the atmosphere, *Nature*, 533(7604), 527–531, doi:10.1038/nature18271,  
 1454 2016.  
 1455  
 1456 Vratolis, S., Gini, M. I., Bezantakos, S., Stavroulas, I., Kalivitis, N., Kostenidou, E., Louvaris, E.,  
 1457 Siakavaras, D., Biskos, G., Mihalopoulos, N., Pandis, S. N. N., Pilinis, C., Papayannis, A. and  
 1458 Eleftheriadis, K.: Particle number size distribution statistics at City-Centre Urban Background, urban  
 1459 background, and remote stations in Greece during summer, *Atmos. Environ.*, 213(May), 711–726,  
 1460 doi:10.1016/j.atmosenv.2019.05.064, 2019.  
 1461  
 1462 [von Bismarck-Osten, C., Birmili, W., Ketzel, M. and Weber, S.: Statistical modelling of aerosol](#)  
 1463 [particle number size distributions in urban and rural environments - A multi-site study, \*Urban\*](#)  
 1464 [Climate, 11\(C\), pp. 51–66. doi: 10.1016/j.uclim.2014.11.004, 2015.](#)  
 1465  
 1466 [von Bismarck-Osten, C. and Weber, S.: A uniform classification of aerosol signature size](#)  
 1467 [distributions based on regression-guided and observational cluster analysis, \*Atmospheric\*](#)  
 1468 [Environment, 89, pp. 346–357. doi: 10.1016/j.atmosenv.2014.02.050, 2014.](#)  
 1469  
 1470 [von Bismarck-Osten, C. Birmili, W., Ketzel, M., Massling, A., Petäjä, T. and Weber, S.:](#)  
 1471 [Characterization of parameters influencing the spatio-temporal variability of urban particle number](#)  
 1472 [size distributions in four European cities, \*Atmospheric Environment\*, 77, pp. 415–429. doi:](#)  
 1473 [10.1016/j.atmosenv.2013.05.029, 2013.](#)  
 1474  
 1475  
 1476 Wagner, P. and Kuttler, W.: Biogenic and anthropogenic isoprene in the near-surface urban  
 1477 atmosphere - A case study in Essen, Germany, *Sci. Total Environ.*, 475, 104–115,  
 1478 doi:10.1016/j.scitotenv.2013.12.026, 2014.  
 1479  
 1480 Wang, D., Fu, Q., Geng, F., Li, L., Wang, H., Qiao, L., Yang, X., Chen, J., Kerminen, V. M.,  
 1481 Petäjä, T., Worsnop, D. R., Kulmala, M. and Wang, L.: Atmospheric new particle formation from  
 1482 sulfuric acid and amines in a Chinese megacity, *Science*, 361(6399), 278–281,  
 1483 doi:10.1126/science.aao4839, 2018.  
 1484  
 1485 Wang, S., Wu, R., Berndt, T., Ehn, M. and Wang, L.: Formation of Highly Oxidized Radicals and  
 1486 Multifunctional Products from the Atmospheric Oxidation of Alkylbenzenes, ,

doi:10.1021/acs.est.7b02374, 2017a.

Wang, Z., Wu, Z., Yue, D., Shang, D., Guo, S., Sun, J., Ding, A., Wang, L., Jiang, J., Guo, H., Gao, J., Cheung, H. C., Morawska, L., Keywood, M. and Hu, M.: New particle formation in China: Current knowledge and further directions, *Sci. Total Environ.*, 577, 258–266, doi:10.1016/j.scitotenv.2016.10.177, 2017b.

Wang, F., Ketzel, M., Ellermann, T., Wählin, P., Jensen, S. S., Fang, D. and Massling, A.: Particle number, particle mass and NO<sub>x</sub> emission factors at a highway and an urban street in Copenhagen, *Atmos. Chem. Phys.*, 10(6), 2745–2764, doi:10.5194/acp-10-2745-2010, 2010.

Wang, M., Kong, W., Marten, R., He, X. C., Chen, D., Pfeifer, J., Heitto, A., Kontkanen, J., Dada, L., Kürten, A., Yli-Juuti, T., Manninen, H. E., Amanatidis, S., Amorim, A., Baalbaki, R., Baccarini, A., Bell, D. M., Bertozzi, B., Bräkling, S., Brilke, S., Murillo, L. C., Chiu, R., Chu, B., De Menezes, L. P., Duplissy, J., Finkenzeller, H., Carracedo, L. G., Granzin, M., Guida, R., Hansel, A., Hofbauer, V., Krechmer, J., Lehtipalo, K., Lamkaddam, H., Lampimäki, M., Lee, C. P., Makhmutov, V., Marie, G., Mathot, S., Mauldin, R. L., Mentler, B., Müller, T., Onnela, A., Partoll, E., Petäjä, T., Philippov, M., Pospisilova, V., Ranjithkumar, A., Rissanen, M., Rörup, B., Scholz, W., Shen, J., Simon, M., Sipilä, M., Steiner, G., Stolzenburg, D., Tham, Y. J., Tomé, A., Wagner, A. C., Wang, D. S., Wang, Y., Weber, S. K., Winkler, P. M., Wlasits, P. J., Wu, Y., Xiao, M., Ye, Q., Zauner-Wieczorek, M., Zhou, X., Volkamer, R., Riipinen, I., Dommen, J., Curtius, J., Baltensperger, U., Kulmala, M., Worsnop, D. R., Kirkby, J., Seinfeld, J. H., El-Haddad, I., Flagan, R. C. and Donahue, N. M.: Rapid growth of new atmospheric particles by nitric acid and ammonia condensation, *Nature*, 581(7807), 184–189, doi:10.1038/s41586-020-2270-4, 2020.

Weber, R. J., McMurry, P. H., Eisele, F. L. and Tanner, D. J.: Measurement of expected nucleation precursor species and 3-500-nm diameter particles at Mauna Loa Observatory, Hawaii, *J. Atmos. Sci.*, 52(12), 2242–2257, doi:10.1175/1520-0469(1995)052<2242:MOENPS>2.0.CO;2, 1995.

Wehner, B., Siebert, H., Stratmann, F., Tuch, T., Wiedensohler, A., Petäjä, T., Dal Maso, M. and Kulmala, M.: Horizontal homogeneity and vertical extent of new particle formation events, *Tellus, Ser. B Chem. Phys. Meteorol.*, 59(3), 362–371, doi:10.1111/j.1600-0889.2007.00260.x, 2007.

Wiedensohler, A., Ma, N., Birmili, W., Heintzenberg, J., Ditas, F., Andreae, M. O. and Panov, A.: Infrequent new particle formation over the remote boreal forest of Siberia, *Atmos. Environ.*, 200, 167–169, doi:10.1016/j.atmosenv.2018.12.013, 2019.

Wonaschütz, A., Demattio, A., Wagner, R., Burkart, J., Zíková, N., Vodička, P., Ludwig, W., Steiner, G., Schwarz, J. and Hitzengerger, R.: Seasonality of new particle formation in Vienna, Austria - Influence of air mass origin and aerosol chemical composition, *Atmos. Environ.*, 118, 118–126,

doi:10.1016/j.atmosenv.2015.07.035, 2015.

1528

Woo, K. S., Chen, D. R., Pui, D. Y. H. H. and McMurry, P. H.: Measurement of Atlanta aerosol size distributions: Observations of ultrafine particle events, *Aerosol Sci. Technol.*, 34, 75–87, doi:10.1080/02786820120056, 2001.

1532

Yamada, H.: Contribution of evaporative emissions from gasoline vehicles toward total VOC emissions in Japan, *Sci. Total Environ.*, 449, 143–149, doi:10.1016/j.scitotenv.2013.01.045, 2013.

1535

Yan, C., Nie, W., Vogel, A. L., Dada, L., Lehtipalo, K., Stolzenburg, D. and Wagner, R.: Size-dependent influence of NO<sub>x</sub> on the growth rates of organic aerosol particles, *Sci. Adv.*, 6, 1–10, 2020.

1539

Yan, C., Dada, L., Rose, C., Jokinen, T., Nie, W., Schobesberger, S., Junninen, H., Lehtipalo, K., Sarnela, N., Makkonen, U., Garmash, O., Wang, Y., Zha, Q., Paasonen, P., Bianchi, F., Sipilä, M., Ehn, M., Petäjä, T., Kerminen, V.-M., Worsnop, D. R. and Kulmala, M.: The role of H<sub>2</sub>SO<sub>4</sub>-NH<sub>3</sub> anion clusters in ion-induced aerosol nucleation mechanisms in the boreal forest, *Atmos. Chem. Phys.*, 18, 13231–13243, doi:10.5194/acp-18-13231-2018, 2018.

1545

Yao, L., Garmash, O., Bianchi, F., Zheng, J., Yan, C., Kontkanen, J., Junninen, H., Mazon, S. B., Ehn, M., Paasonen, P., Sipilä, M., Wang, M., Wang, X., Xiao, S., Chen, H., Lu, Y., Zhang, B., Wang, M., Chen, D., Xiao, M., Ye, Q., Stolzenburg, D., Hofbauer, V., Ye, P., Vogel, A. L., Mauldin, R. L., Amorim, A., Baccarini, A., Baumgartner, B., Brilke, S., Dada, L., Dias, A., Duplissy, J., Finkenzeller, H., Garmash, O., He, X. C., Hoyle, C. R., Kim, C., Kvashnin, A., Lehtipalo, K., Fischer, L., Molteni, U., Petäjä, T., Pospisilova, V., Quéléver, L. L. J., Rissanen, M., Simon, M., Tauber, C., Tomé, A., Wagner, A. C., Weitz, L., Volkamer, R., Winkler, P. M., Kirkby, J., Worsnop, D. R., Kulmala, M., Baltensperger, U., Dommen, J., El-Haddad, I. and Donahue, N. M.: Photo-oxidation of Aromatic Hydrocarbons Produces Low-Volatility Organic Compounds, *Environ. Sci. Technol.*, 54(13), 7911–7921, doi:10.1021/acs.est.0c02100, 2020.

1556

Ye, J., Abbatt, J. P. D., Chan, A. W.H., Novel pathway of SO<sub>2</sub> oxidation in the atmosphere: reactions with monoterpene ozonolysis intermediates and secondary organic aerosol, *Atmos. Chem. Phys.*, 18, 5549–5565, 2018

Yli-Juuti, T., Mohr, C. and Riipinen, I.: Open questions on atmospheric nanoparticle growth, *Commun. Chem.*, 3(1), 2–5, doi:10.1038/s42004-020-00339-4, 2020.

1562

Zhang, R., Khalizov, A., Wang, L., Hu, M. and Xu, W.: Nucleation and growth of nanoparticles in the atmosphere, *Chem. Rev.*, 112(3), 1957–2011, doi:10.1021/cr2001756, 2012.

1565

1566



1567 **TABLE LEGENDS**

1568

1569 **Table 1:** Location and data availability of the sites.

1570

1571 **Table 2:** Frequency (and number of NPF events), growth and formation rate of NPF events.

1572

1573 **Table 3:** Normalised gradients (non-normalised for growth rate),  $R^2$  and p-values (- for values  
1574  $>0.05$ ) for the relationship between meteorological conditions and NPF event  
1575 variables. Gradients of  $R^2 > 0.50$  are in bold.

1576

1577 **Table 4:** Normalised gradients (non-normalised for growth rate),  $R^2$  and p-values (- for values  
1578  $>0.05$ ) for the relationship between atmospheric composition variables and NPF  
1579 event variables. Gradients of  $R^2 > 0.50$  are in bold.

1580

1581

1582 **FIGURE LEGENDS**

1583

1584 **Figure 1:** Map of the sites of the present study.

1585

1586 **Figure 2:** Relation of average downward incoming solar radiation ( $K_{\downarrow}$ ) and normalised  
1587 gradients  $a_N^*$ .

1588

1589 **Figure 3:** Normalised gradients  $a_J^*$  for  $K_{\downarrow}$  (\*UK sites are calculated with solar irradiance).

1590

1591 **Figure 4a:** Relationship of average relative humidity and normalised gradients  $a_N^*$ .

1592

1593 ~~**Figure 4b:** Relationship of average relative humidity and normalised gradients  $a_N^*$  (SPAUB not~~  
1594 ~~included).~~

1595

1596 **Figure 5:** Relationship of average temperature and normalised gradients  $a_N^*$ .

1597

1598 **Figure 6:** Normalised gradients  $a_J^*$  for temperature.

1599

1600 **Figure 7a:** Relationship of average  $SO_2$  concentrations and normalised gradients  $a_N^*$  for the  
1601 sites with available data (a) and for the sites with available data excluding UKRO  
1602 (b).

1603

1604 ~~**Figure 7b:** Relationship of average  $SO_2$  concentrations and normalised gradients  $a_N^*$  (UKRO~~  
1605 ~~not included).~~

1606

1607 **Figure 8:** Relationship of average O<sub>3</sub> concentrations and normalised gradients  $a_N^*$ .

**Table 1:** Location and data availability of the sites.

Site	Location	Available data	Meteorological data location	Data availability	Reference
<b>UKRU</b>	Harwell Science Centre, Oxford, 80 km W of London, UK (51° 34' 15" N; 1° 19' 31" W)	SMPS (16.6 - 604 nm, 76.5% availability), NO <sub>x</sub> , SO <sub>2</sub> , O <sub>3</sub> , OC, SO <sub>4</sub> <sup>2-</sup> , gaseous ammonia	On site	2009 - 2015	Charron et al., 2013
<b>UKUB</b>	North Kensington, 4 km W of London city centre, UK (51° 31' 15" N; 0° 12' 48" W)	SMPS (16.6 - 604 nm, 83.3% availability), NO <sub>x</sub> , SO <sub>2</sub> , O <sub>3</sub> , OC, SO <sub>4</sub> <sup>2-</sup>	Heathrow airport	2009 - 2015	Bigi and Harrison, 2010
<b>UKRO</b>	Marylebone Road, London, UK (51° 31' 21" N; 0° 9' 16" W)	SMPS (16.6 - 604 nm, 74.3% availability), NO <sub>x</sub> , SO <sub>2</sub> , O <sub>3</sub> , OC, SO <sub>4</sub> <sup>2-</sup>	Heathrow airport	2009 - 2015	Charron and Harrison, 2003
<b>DENRU</b>	Lille Valby, 25 km W of Copenhagen, (55° 41' 41" N; 12° 7' 7" E) (2008 – 6/2010) Risø, 7 km north of Lille Valby, (55° 38' 40" N; 12° 5' 19" E) (7/2010 – 2017)	DMPS and CPC (5.8 - 700 nm, 68.3% availability), NO <sub>x</sub> , SO <sub>2</sub> , O <sub>3</sub> , OC, SO <sub>4</sub> <sup>2-</sup>	H.C. Ørsted – Institute station	2008 – 2017	Ketzel et al., 2004
<b>DENUB</b>	H.C. Ørsted – Institute, 2 km NE of the city centre, Copenhagen, Denmark (55° 42' 1" N; 12° 33' 41" E)	DMPS and CPC (5.8 - 700 nm, 61.4% availability), NO <sub>x</sub> , O <sub>3</sub>	On site	2008 – 2017	Wang et al., 2010
<b>DENRO</b>	H.C. Andersens Boulevard, Copenhagen, Denmark (55° 40' 28" N; 12° 34' 16" E)	DMPS and CPC (5.8 - 700 nm, 65.7% availability), NO <sub>x</sub> , SO <sub>2</sub> , O <sub>3</sub> , OC, SO <sub>4</sub> <sup>2-</sup>	H.C. Ørsted – Institute station	2008 – 2017	Wang et al., 2010
<b>GERRU</b>	Melpitz, 40 km NE of Leipzig, Germany (51° 31' 31.85" N; 12° 26' 40.30" E)	TDMPs with CPC (4.8 - 800 nm, 87.2% availability), OC, SO <sub>4</sub> <sup>2-</sup>	On site	2008 – 2011	Birmili et al., 2016
<b>GERUB</b>	Tropos, 3 km NE from the city centre of Leipzig, Germany (51° 21' 9.1" N; 12° 26' 5.1" E)	TDMPs with CPC (3 - 800 nm, 90.4% availability)	On site	2008 – 2011	Birmili et al., 2016
<b>GERRO</b>	Eisenbahnstraße, Leipzig, Germany (51° 20' 43.80" N; 12° 24' 28.35" E)	TDMPs with CPC (4 - 800 nm, 68.3% availability)	Tropos station	2008 – 2011	Birmili et al., 2016
<b>FINRU</b>	Hyttiälä, 250 km N of Helsinki, Finland (61° 50' 50.70" N; 24° 17' 41.20" E)	TDMPs with CPC (3 – 1000 nm, 98.2% availability), NO <sub>x</sub> , SO <sub>2</sub> , O <sub>3</sub> , VOCs	On site	2008 – 2011 & 2015 – 2018	Aalto et al., 2001
<b>FINUB</b>	Kumpula Campus 4 km N of the city centre, Helsinki, Finland (60° 12' 10.52" N; 24° 57' 40.20" E)	TDMPs with CPC (3.4 - 1000 nm, 99.7% availability)	On site	2008 – 2011 & 2015 – 2018	Järvi et al., 2009
<b>FINRO</b>	Mäkelänkatu street, Helsinki, Finland (60° 11' 47.57" N; 24° 57' 6.01" E)	DMPS (6 - 800 nm, 90.0% availability), NO <sub>x</sub> , O <sub>3</sub>	Pasila station and on site	2015 – 2018	Hietikko et al., 2018
<b>SPARU</b>	Montseny, 50 km NNE from Barcelona, Spain (41° 46' 45" N; 2° 21' 29" E)	SMPS (9 – 856 nm, 53.7% availability), NO <sub>2</sub> , SO <sub>2</sub> , O <sub>3</sub>	On site	2012 - 2015	Dall'Osto et al., 2013
<b>SPAUB</b>	Palau Reial, Barcelona, Spain (41° 23' 14" N; 2° 6' 56" E)	SMPS (11 – 359 nm, 88.1% availability), NO <sub>2</sub> , SO <sub>2</sub> , O <sub>3</sub>	On site	2012 – 2015	Dall'Osto et al., 2012
<b>GRERU</b>	Finokalia, 70 km E of Heraklion, Greece (35° 20' 16.8" N; 25° 40' 8.4" E)	SMPS (8.77 - 849 nm, 85.0% availability), NO <sub>2</sub> , O <sub>3</sub> , OC	On site	2012 – 2018	Kalkavouras et al., 2017
<b>GREUB</b>	"Demokritos", 12 km NE from the city centre, Athens, Greece (37° 59' 41.96" N; 23° 48' 57.56" E)	SMPS (10 – 550 nm, 88.0% availability)	On site	2015 – 2018	Mølgaard et al., 2013

1610 **Table 2:** Frequency (and number of NPF events), growth and formation rate of [class 1a](#) NPF events.

Site	Frequency of NPF events (%)	GR (nm h <sup>-1</sup> )	J <sub>10</sub> (N cm <sup>-3</sup> s <sup>-1</sup> )
<b>UKRU</b>	7.0 (160)	3.4*	8.69E-03**
<b>UKUB</b>	7.0 (156)	4.2*	1.42E-02**
<b>UKRO</b>	6.1 (120)	5.5*	3.75E-02**
<b>DENRU</b>	7.9 (176)	3.19	2.57E-02
<b>DENUB</b>	5.8 (116)	3.19	2.40E-02
<b>DENRO</b>	5.4 (117)	4.45	8.07E-02
<b>GERRU</b>	17.1 (164)	4.34	9.18E-02
<b>GERUB</b>	17.5 (169)	4.24	1.02E-01
<b>GERRO</b>	9.0 (62)	5.17	1.38E-01
<b>FINRU</b>	8.7 (190)	2.91	1.19E-02
<b>FINUB</b>	5.0 (110)	2.87	2.49E-02
<b>FINRO</b>	5.1 (49)	3.74	6.94E-02
<b>SPARU</b>	12 (68)	3.87	1.54E-02
<b>SPAUB</b>	13.1 (97)	3.71	2.12E-02
<b>GRERU</b>	6.5 (116)	3.68	4.90E-03
<b>GREUB</b>	8.5 (82)	3.4	4.41E-02

\* GR up to 50 nm calculated

\*\* J<sub>16</sub> calculated

**Table 3:** Normalised gradients (non-normalised for growth rate),  $R^2$  and p-values (- for values  $>0.05$ ) for the relation between meteorological conditions and NPF event variables. Gradients of  $R^2 > 0.50$  are in bold.

Downward shortwave solar radiation $K_{\downarrow}$ ( $W\ m^{-2}$ )										
Site	$a_N^*$ ( $W^{-1}\ m^2$ )	$R^2$	p	$a_G$	$R^2$	p	$a_J^*$ ( $W^{-1}\ m^2$ )	$R^2$	p	Average
UKRU*	<b>1.21E-03</b>	0.94	<0.001	6.53E-05	0.11	-	<b>6.28E-04</b>	0.93	<0.001	443
UKUB*	<b>6.81E-04</b>	0.90	<0.001	-8.26E-05	0.10	-	1.49E-04	0.19	-	448
UKRO*	<b>8.69E-04</b>	0.98	<0.001	-7.75E-06	0.00	-	<b>2.66E-04</b>	0.64	<0.005	464
DENRU	<b>2.22E-03</b>	0.88	<0.001	4.24E-04	0.20	-	<b>1.38E-03</b>	0.64	<0.001	115
DENUB	<b>1.87E-03</b>	0.91	<0.001	1.47E-04	0.03	-	8.98E-04	0.48	<0.01	115
DENRO	<b>2.46E-03</b>	0.95	<0.001	1.27E-04	0.01	-	<b>6.77E-04</b>	0.50	<0.005	117
GERRU	<b>2.87E-03</b>	0.98	<0.001	<b>9.88E-04</b>	0.72	<0.01	<b>1.45E-03</b>	0.81	<0.001	130
GERUB	<b>3.18E-03</b>	0.97	<0.001	<b>7.28E-04</b>	0.51	<0.005	<b>1.53E-03</b>	0.69	<0.001	114
GERRO	<b>2.40E-03</b>	0.95	<0.001	-5.89E-04	0.09	-	<b>9.95E-04</b>	0.59	<0.005	114
FINRU	<b>2.63E-03</b>	0.76	<0.001	<b>1.01E-03</b>	0.57	<0.01	<b>2.04E-03</b>	0.82	<0.001	91.5
FINUB	1.38E-03	0.37	-	1.81E-04	0.08	-	8.99E-04	0.25	-	111
FINRO	<b>1.76E-03</b>	0.59	<0.005	9.15E-04	0.34	<0.005	4.45E-04	0.03	-	114
SPARU	3.46E-04	0.35	<0.05	5.68E-04	0.13	-	<b>1.97E-03</b>	0.74	<0.001	162
SPAUB	<b>5.92E-04</b>	0.58	<0.05	6.98E-04	0.23	-	<b>1.58E-03</b>	0.81	<0.001	180
GRERU	<b>4.10E-04</b>	0.52	<0.001	<b>7.14E-04</b>	0.55	<0.001	-6.30E-04	0.05	-	201
GREUB	3.49E-04	0.31	-	-1.10E-04	0.02	-	8.97E-04	0.34	<0.05	183

\* Global solar irradiation measurements in  $kJ\ m^{-2}$

Relative Humidity (%)										
Site	$a_N^*$ ( $\%^{-1}$ )	$R^2$	p	$a_G$	$R^2$	p	$a_J^*$ ( $\%^{-1}$ )	$R^2$	p	Average
UKRU	<b>-5.89E-02</b>	0.85	<0.001	1.69E-03	0.02	-	<b>-3.35E-02</b>	0.85	<0.001	79.7
UKUB	<b>-3.42E-02</b>	0.94	<0.001	8.23E-03	0.24	-	-5.66E-03	0.19	-	75.3
UKRO	<b>-5.09E-02</b>	0.85	<0.001	7.03E-03	0.25	-	-1.49E-02	0.46	<0.05	74.5
DENRU	<b>-3.90E-02</b>	0.95	<0.001	<b>9.42E-03</b>	0.74	<0.001	5.45E-04	0.00	-	75.7
DENUB	<b>-3.14E-02</b>	0.94	<0.001	3.64E-03	0.06	-	2.57E-03	0.00	-	75.7
DENRO	<b>-3.64E-02</b>	0.95	<0.001	-1.21E-02	0.22	-	-3.91E-03	0.10	-	75.7
GERRU	<b>-5.08E-02</b>	0.88	<0.001	<b>-1.30E-02</b>	0.72	<0.001	<b>-2.46E-02</b>	0.91	<0.001	81.9
GERUB	<b>-5.35E-02</b>	0.86	<0.001	<b>-6.34E-03</b>	0.67	<0.001	<b>-2.25E-02</b>	0.86	<0.001	78.7
GERRO	<b>-2.83E-02</b>	0.90	<0.001	3.98E-03	0.05	-	<b>-1.72E-02</b>	0.81	<0.001	78.7
FINRU	<b>-4.48E-02</b>	0.94	<0.001	<b>-7.07E-03</b>	0.65	<0.001	<b>-2.16E-02</b>	0.87	<0.001	80.1
FINUB	<b>-5.89E-02</b>	0.95	<0.001	1.04E-02	0.26	-	-6.52E-03	0.18	-	76.5
FINRO	<b>-3.34E-02</b>	0.92	<0.001	-1.47E-03	0.01	-	7.39E-03	0.10	-	71.1
SPARU	<b>-1.54E-02</b>	0.90	<0.001	-4.67E-03	0.08	-	-7.12E-03	0.14	-	66.4
SPAUB	<b>-4.84E-02</b>	0.93	<0.001	<b>2.43E+02</b>	0.50	<0.01	-9.83E-03	0.19	-	69.2
GRERU	-7.72E-03	0.22	-	1.06E-02	0.06	-	-1.83E-01	0.15	-	70.0
GREUB	<b>-1.42E-02</b>	0.62	<0.001	2.83E-03	0.06	-	4.85E-04	0.00	-	60.5

Temperature (°C)										
Site	a <sub>N</sub> * (°C <sup>-1</sup> )	R <sup>2</sup>	P	a <sub>G</sub>	R <sup>2</sup>	P	a <sub>J</sub> * (°C <sup>-1</sup> )	R <sup>2</sup>	P	Average
UKRU	<b>1.10E-01</b>	0.93	<0.001	<b>7.85E-02</b>	0.94	<0.001	<b>8.72E-02</b>	0.84	<0.001	10.6
UKUB	<b>9.04E-02</b>	0.98	<0.001	<b>1.39E-01</b>	0.96	<0.001	<b>6.34E-02</b>	0.73	<0.005	11.8
UKRO	<b>8.22E-02</b>	0.98	<0.001	<b>3.51E-02</b>	0.52	<0.05	4.32E-02	0.44	<0.05	12.1
DENRU	<b>6.68E-02</b>	0.83	<0.001	1.54E-02	0.08	-	<b>6.68E-02</b>	0.92	<0.001	9.80
DENUB	<b>2.50E-02</b>	0.45	<0.05	2.40E-02	0.33	-	3.05E-02	0.45	<0.05	9.82
DENRO	<b>6.64E-02</b>	0.88	<0.001	3.51E-03	0.00	-	<b>2.96E-02</b>	0.58	<0.005	10.0
GERRU	<b>7.27E-02</b>	0.92	<0.001	<b>5.65E-02</b>	0.92	<0.001	<b>5.37E-02</b>	0.93	<0.001	10.3
GERUB	<b>8.20E-02</b>	0.93	<0.001	<b>3.38E-02</b>	0.62	<0.001	<b>4.28E-02</b>	0.54	<0.005	11.1
GERRO	<b>5.08E-02</b>	0.89	<0.001	-3.33E-03	0.00	-	1.61E-02	0.11	-	11.1
FINRU	-2.01E-02	0.17	-	<b>1.13E-01</b>	0.79	<0.001	<b>4.27E-02</b>	0.72	<0.001	4.79
FINUB	-4.21E-03	0.00	-	<b>7.42E-02</b>	0.83	<0.001	1.67E-02	0.28	-	6.52
FINRO	<b>6.24E-02</b>	0.65	<0.005	<b>9.28E-02</b>	0.87	<0.001	-1.09E-02	0.05	-	7.72
SPARU	-2.51E-02	0.41	<0.05	<b>1.23E-01</b>	0.92	<0.001	<b>9.11E-02</b>	0.71	<0.001	13.9
SPAUB	-3.43E-03	0.02	-	<b>6.67E-02</b>	0.66	<0.005	1.18E-02	0.08	-	18.2
GRERU	<b>-4.66E-02</b>	0.75	<0.001	<b>1.74E-01</b>	0.75	<0.001	-9.45E-02	0.47	<0.05	18.2
GREUB	-1.00E-02	0.25	-	<b>4.67E-02</b>	0.62	<0.005	-2.85E-02	0.20	-	17.6

Wind Speed (m s <sup>-1</sup> )										
Site	a <sub>N</sub> * (m <sup>-1</sup> s)	R <sup>2</sup>	P	a <sub>G</sub>	R <sup>2</sup>	P	a <sub>J</sub> * (m <sup>-1</sup> s)	R <sup>2</sup>	P	Average
UKRU	5.72E-02	0.20	-	-3.04E-02	0.07	-	6.87E-03	0.00	-	3.96
UKUB	<b>1.72E-01</b>	0.87	<0.001	<b>-1.91E-01</b>	0.71	<0.001	3.56E-03	0.00	-	4.16
UKRO	6.34E-02	0.19	-	3.21E-02	0.02	-	7.28E-02	0.45	<0.005	4.14
DENRU	<b>1.08E-01</b>	0.88	<0.001	<b>-2.33E-01</b>	0.74	<0.001	1.28E-01	0.44	<0.01	4.17
DENUB	<b>1.50E-01</b>	0.90	<0.001	-3.33E-02	0.10	-	8.31E-02	0.19	-	4.17
DENRO	<b>1.65E-01</b>	0.89	<0.001	-1.51E-01	0.49	<0.001	9.08E-03	0.00	-	4.16
GERRU	<b>-1.06E-01</b>	0.57	<0.005	<b>-2.26E-01</b>	0.83	<0.001	-5.32E-03	0.00	-	2.58
GERUB	<b>-1.27E-01</b>	0.52	<0.01	<b>-1.41E-01</b>	0.60	<0.005	-3.32E-02	0.04	-	2.33
GERRO	<b>-2.40E-01</b>	0.56	-	-2.54E-01	0.38	-	-1.30E-01	0.22	-	2.33
FINRU	<b>1.62E-01</b>	0.63	<0.005	-1.29E-01	0.16	<0.05	7.99E-02	0.07	-	1.31
FINUB	-3.17E-02	0.08	-	7.26E-02	0.20	<0.05	-9.74E-02	0.17	-	3.43
FINRO	<b>8.62E-02</b>	0.51	<0.05	-1.60E-01	0.32	<0.05	-1.86E-01	0.32	-	4.26
SPARU	-2.20E-02	0.02	-	3.80E-01	0.31	-	5.74E-02	0.02	-	0.94
SPAUB	<b>2.90E-01</b>	0.93	<0.001	7.71E-02	0.24	-	-5.90E-02	0.05	-	2.05
GRERU	<b>4.37E-02</b>	0.54	<0.001	1.01E-01	0.36	<0.005	1.73E-03	0.00	-	6.06
GREUB	-1.13E-01	0.47	<0.01	<b>-1.88E-01</b>	0.50	<0.005	-3.78E-02	0.01	-	1.87

1620

Atmospheric Pressure (mbar)										
Site	a <sub>N</sub> * (mbar <sup>-1</sup> )	R <sup>2</sup>	p	a <sub>G</sub>	R <sup>2</sup>	p	a <sub>J</sub> * (mbar <sup>-1</sup> )	R <sup>2</sup>	p	Average
UKRU	4.26E-02	0.83	<0.005	3.93E-02	0.58	<0.005	2.95E-02	0.47	<0.05	1007.7
UKUB	1.90E-02	0.50	-	1.17E-02	0.05	<0.05	4.16E-03	0.04	-	1011.7
UKRO	6.33E-02	0.95	<0.001	-1.21E-01	0.40	-	-2.98E-02	0.17	-	1012
GERRU	5.10E-02	0.97	-	8.95E-02	0.85	<0.001	2.16E-02	0.21	-	1007.0
GERUB	6.27E-02	0.97	-	4.00E-02	0.76	-	2.00E-02	0.37	<0.05	995.5
GERRO	4.57E-02	0.79	-	-9.61E-02	0.43	-	-2.80E-02	0.21	-	995.5
FINRU	3.46E-02	0.88	<0.001	2.90E-02	0.57	<0.001	1.05E-02	0.14	-	985.1
FINUB	2.61E-02	0.55	<0.005	-3.57E-03	0.02	-	4.38E-03	0.05	-	1004.4
FINRO	4.91E-02	0.70	-	-2.67E-02	0.17	-	1.43E-02	0.26	-	1008.8
SPARU	-2.02E-02	0.09	-	4.79E-02	0.14	-	2.89E-02	0.08	-	939.3
SPAUB	-2.83E-02	0.44	<0.05	1.86E-02	0.08	-	1.68E-02	0.21	-	1006.3
GRERU	6.00E-02	0.46	<0.001	-1.50E-01	0.73	-	8.14E-02	0.33	-	1014.5
GREUB	9.42E-03	0.10	<0.05	-1.00E-01	0.71	-	1.58E-02	0.04	-	1015.7

1625

**Table 4:** Normalised gradients (non-normalised for growth rate), R<sup>2</sup> and p-values (- for values >0.05) for the relation between atmospheric composition variables and NPF event variables. Gradients of R<sup>2</sup> > 0.50 are in bold.

SO <sub>2</sub> (µg m <sup>-3</sup> )										
Site	a <sub>N</sub> * (µg <sup>-1</sup> m <sup>3</sup> )	R <sup>2</sup>	p	a <sub>G</sub>	R <sup>2</sup>	p	a <sub>J</sub> * (µg <sup>-1</sup> m <sup>3</sup> )	R <sup>2</sup>	p	Average
UKRU	-1.97E-01	0.38	<0.05	-6.17E-02	0.02	-	3.30E-01	0.06	-	1.64
UKUB	<b>-2.57E-01</b>	0.62	<0.001	1.93E-02	0.00	-	4.18E-01	0.40	-	2.04
UKRO	<b>-1.03E-01</b>	0.82	<0.001	6.90E-02	0.34	<0.01	<b>8.43E-02</b>	0.77	<0.001	7.46
DENRU	<b>-9.77E-01</b>	0.53	<0.05	2.84E+00	0.37	-	4.38E-01	0.09	-	0.52
DENRO	<b>-4.20E-01</b>	0.91	<0.001	<b>6.42E-01</b>	0.54	<0.005	<b>5.66E-01</b>	0.62	<0.001	0.97
FINRU	-5.66E-01	0.05	-	-1.42E+00	0.19	-	-6.30E-02	0.00	-	0.09
SPARU	<b>-3.62E-01</b>	0.74	<0.001	-1.33E-01	0.02	-	-3.55E-02	0.01	-	0.95
SPAUB	-2.93E-02	0.04	-	<b>4.12E-01</b>	0.59	-	1.07E-01	0.29	-	1.99

NO <sub>x</sub> or NO <sub>2</sub> (ppb)										
Site	a <sub>N</sub> * (ppb <sup>-1</sup> )	R <sup>2</sup>	p	a <sub>G</sub>	R <sup>2</sup>	p	a <sub>J</sub> * (ppb <sup>-1</sup> )	R <sup>2</sup>	p	Average
UKRU	<b>-4.99E-02</b>	0.67	<0.005	<b>4.52E-02</b>	0.58	<0.05	<b>-4.51E-02</b>	0.70	<0.005	11.7
UKUB	<b>-8.75E-03</b>	0.83	<0.001	-3.97E-04	0.00	-	-1.09E-02	0.43	<0.05	53.6
UKRO	<b>-3.22E-03</b>	0.72	<0.001	1.44E-03	0.39	<0.05	<b>2.19E-03</b>	0.66	<0.001	299
DENRU	-9.41E-02	0.43	<0.005	-4.89E-03	0.00	<0.001	<b>-6.47E-02</b>	0.55	<0.01	5.42
DENUB	<b>-4.99E-02</b>	0.68	<0.001	2.85E-02	0.26	-	8.55E-04	0.00	-	10.5
DENRO	<b>-5.10E-03</b>	0.75	<0.001	<b>1.10E-02</b>	0.69	<0.001	<b>8.33E-03</b>	0.88	<0.001	68.5
FINRU	<b>-7.27E-01</b>	0.54	<0.001	-2.74E-01	0.11	-	1.95E-01	0.05	-	0.72
FINRO	<b>-6.24E-03</b>	0.68	<0.001	1.70E-03	0.12	-	3.25E-03	0.03	-	88.1
SPARU*	-1.53E-02	0.05	-	2.54E-02	0.01	-	1.25E-01	0.21	-	3.26
SPAUB*	<b>-2.59E-02</b>	0.62	<0.005	<b>2.23E-02</b>	0.70	<0.001	2.57E-03	0.01	-	31.4
GRERU*	3.01E-01	0.19	-	<b>-1.40E+00</b>	0.75	<0.001	5.23E-01	0.13	-	0.52

1630 \* NO<sub>2</sub> measurements



O <sub>3</sub> (ppb)										
Site	a <sub>N</sub> * (ppb <sup>-1</sup> )	R <sup>2</sup>	p	a <sub>G</sub>	R <sup>2</sup>	p	a <sub>J</sub> * (ppb <sup>-1</sup> )	R <sup>2</sup>	p	Average
UKRU	<b>2.27E-02</b>	0.88	<0.001	<b>-4.89E-02</b>	0.53	<0.005	-3.53E-03	0.01	-	54.4
UKUB	<b>1.37E-02</b>	0.87	<0.001	<b>-3.45E-02</b>	0.68	<0.001	-5.95E-03	0.05	-	39.3
UKRO	<b>7.46E-02</b>	0.95	<0.001	-1.06E-02	0.09	-	<b>-2.44E-02</b>	0.63	<0.005	16.2
DENRU	<b>4.97E-02</b>	0.92	<0.001	-1.32E-02	0.15	-	1.23E-02	0.08	-	30.1
DENUB	<b>5.85E-02</b>	0.84	<0.001	<b>-1.69E-02</b>	0.58	-	2.77E-02	0.32	<0.05	28.2
DENRO	<b>6.42E-02</b>	0.51	<0.05	1.39E-02	0.03	-	<b>3.24E-02</b>	0.91	<0.05	31.1
FINRU	<b>6.76E-02</b>	0.77	<0.05	<b>-4.23E-02</b>	0.60	-	3.92E-02	0.37	<0.05	27.4
FINRO	<b>2.38E-02</b>	0.91	<0.001	6.11E-03	0.24	-	-1.83E-02	0.29	-	37.1
SPARU	1.57E-02	0.02	-	4.34E-02	0.11	-	1.31E-02	0.31	-	75.9
SPAUB	7.99E-03	0.38	<0.05	-5.83E-03	0.30	-	-1.13E-03	0.01	-	54.9
GRERU	7.55E-03	0.04	-	3.68E-02	0.17	-	-3.01E-02	0.15	-	49.5

Particulate Organic Carbon (µg m <sup>-3</sup> )										
Site	a <sub>N</sub> * (µg <sup>-1</sup> m <sup>3</sup> )	R <sup>2</sup>	p	a <sub>G</sub>	R <sup>2</sup>	p	a <sub>J</sub> * (µg <sup>-1</sup> m <sup>3</sup> )	R <sup>2</sup>	p	Average
UKRU	-3.30E-02	0.00	-	1.13E+00	0.42	<0.005	2.13E-01	0.16	-	1.96
UKUB	<b>-2.76E-01</b>	0.59	<0.005	<b>6.63E-01</b>	0.58	<0.05	<b>2.19E-01</b>	0.55	<0.05	3.63
UKRO	<b>-3.78E-01</b>	0.89	<0.001	<b>8.12E-01</b>	0.57	<0.005	<b>4.60E-01</b>	0.75	<0.001	6.24
DENRU	<b>-4.44E-01</b>	0.75	<0.001	2.24E-01	0.11	-	<b>-3.17E-01</b>	0.68	<0.01	1.48
DENRO	-7.80E-02	0.11	-	<b>1.10E+00</b>	0.77	<0.005	<b>4.02E-01</b>	0.81	<0.005	2.59
GERRU	-1.26E-01	0.24	-	1.35E-01	0.09	-	3.14E-02	0.03	-	2.18
FINRU	2.27E-02	0.00	-	<b>3.39E-01</b>	0.60	<0.005	-3.46E-01	0.16	-	1.78
GRERU	-2.08E-01	0.11	-	7.87E-01	0.41	<0.05	8.94E-01	0.11	-	1.58

Sulphate (µg m <sup>-3</sup> )										
Site	a <sub>N</sub> * (µg <sup>-1</sup> m <sup>3</sup> )	R <sup>2</sup>	p	a <sub>G</sub>	R <sup>2</sup>	p	a <sub>J</sub> * (µg <sup>-1</sup> m <sup>3</sup> )	R <sup>2</sup>	p	Average
UKRU <sup>1</sup>	<b>-2.62E-01</b>	0.57	<0.001	<b>7.34E-01</b>	0.77	<0.001	7.99E-01	0.44	<0.05	1.97
UKUB <sup>1</sup>	<b>-3.57E-01</b>	0.89	<0.001	9.28E-01	0.44	<0.01	9.72E-01	0.16	-	1.58
UKRO <sup>1</sup>	-6.05E-02	0.24	-	3.04E-01	0.34	<0.05	-6.22E-02	0.04	-	1.98
DENRU <sup>2</sup>	-7.81E-01	0.34	<0.05	<b>1.02E+00</b>	0.60	<0.05	<b>-1.03E+00</b>	0.63	<0.01	0.52
DENRO <sup>2</sup>	-8.23E-01	0.28	-	1.99E+00	0.22	-	2.82E-01	0.12	-	0.55
GERRU <sup>1</sup>	-3.37E-02	0.00	-	5.89E-01	0.11	-	-4.89E-02	0.01	-	0.92
FINRU <sup>3</sup>	<b>-1.18E+00</b>	0.65	<0.001	2.35E-01	0.09	-	-2.53E-01	0.17	-	1.02

<sup>1</sup> Measurements in PM<sub>10</sub>

<sup>2</sup> Measurements in PM<sub>2.5</sub>

<sup>3</sup> Measurements in PM<sub>1</sub>

Condensation Sink (s <sup>-1</sup> )										
Site	a <sub>N</sub> * (s)	R <sup>2</sup>	P	a <sub>G</sub>	R <sup>2</sup>	P	a <sub>J</sub> * (s)	R <sup>2</sup>	P	Average
UKRU	<b>-2.28E+02</b>	0.72	<0.001	<b>2.64E+02</b>	0.60	<0.001	7.58E+01	0.22	-	3.38E-03
UKUB	<b>-1.66E+02</b>	0.78	<0.001	2.49E+02	0.41	<0.05	1.73E+02	0.35	<0.05	7.41E-03
UKRO	<b>-4.03E+01</b>	0.75	<0.001	2.33E+01	0.18	-	<b>8.94E+01</b>	0.91	<0.001	2.12E-02
DENRU	<b>-4.48E+01</b>	0.91	<0.001	6.90E+01	0.49	<0.05	5.37E+01	0.24	-	9.46E-03
DENUB	<b>-3.78E+01</b>	0.75	<0.001	3.58E+01	0.25	-	1.55E+01	0.56	<0.005	1.42E-02
DENRO	<b>-1.06E+01</b>	0.73	<0.001	<b>2.53E+01</b>	0.56	<0.005	<b>2.72E+01</b>	0.79	<0.001	3.10E-02
GERRU	<b>1.54E+02</b>	0.86	<0.001	<b>1.33E+02</b>	0.56	<0.001	<b>6.67E+01</b>	0.63	<0.001	7.02E-03
GERUB	<b>3.59E+01</b>	0.56	<0.005	3.63E+01	0.17	-	<b>4.74E+01</b>	0.75	<0.001	9.11E-03
GERRO	3.89E+01	0.22	<0.05	-2.21E+01	0.03	<0.005	3.54E+01	0.45	<0.005	1.20E-02
FINRU	<b>-1.80E+02</b>	0.59	<0.005	<b>4.01E+02</b>	0.74	<0.001	4.98E+01	0.10	-	2.32E-03
FINUB	<b>-1.51E+02</b>	0.63	<0.005	8.14E+01	0.31	-	2.01E+02	0.41	<0.05	6.34E-03
FINRO	<b>-6.99E+01</b>	0.77	<0.001	-1.56E+01	0.05	-	<b>2.42E+02</b>	0.83	<0.001	8.96E-03
SPARU	<b>-2.15E+02</b>	0.65	<0.005	1.86E+01	0.00	-	8.60E+01	0.47	<0.05	5.49E-03
SPAUB	<b>-1.18E+02</b>	0.65	<0.005	3.74E+01	0.38	<0.05	<b>9.51E+01</b>	0.52	<0.01	1.00E-02
GRERU	4.33E+00	0.00	-	<b>2.86E+02</b>	0.70	<0.001	<b>1.77E+02</b>	0.56	<0.005	4.66E-03
GREUB	<b>1.64E+02</b>	0.65	<0.001	9.31E+01	0.28	<0.05	<b>1.73E+02</b>	0.83	<0.001	7.55E-03

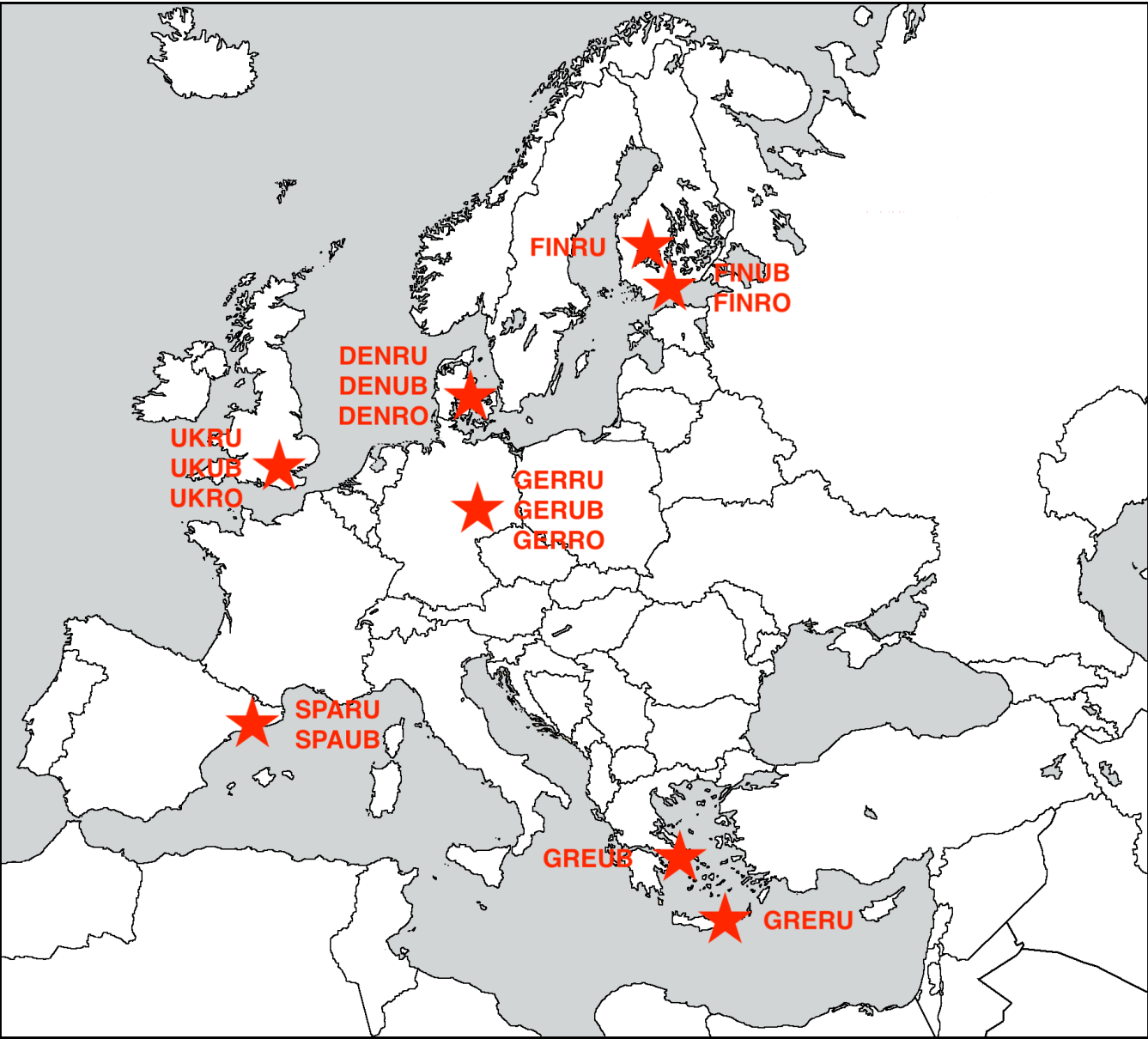


**Figure 1:** Map of the sites of the present study.

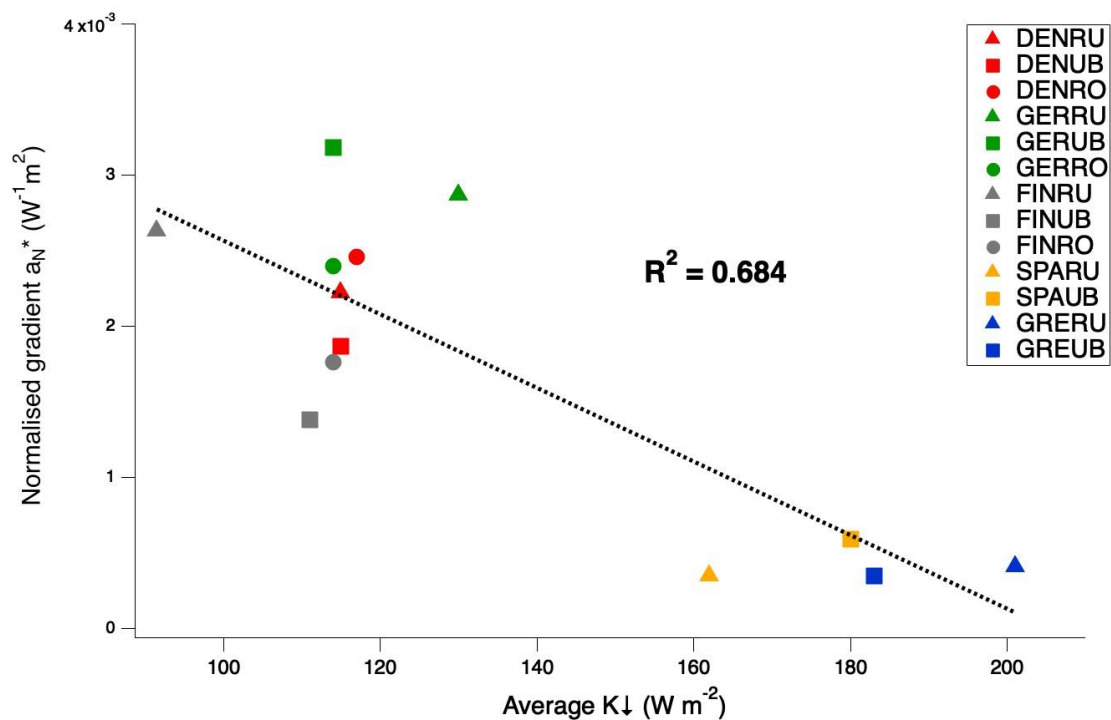


**Figure 2:** Relationship of average downward incoming solar radiation ( $K_{\downarrow}$ ) and normalised gradients  $a_N^*$ .

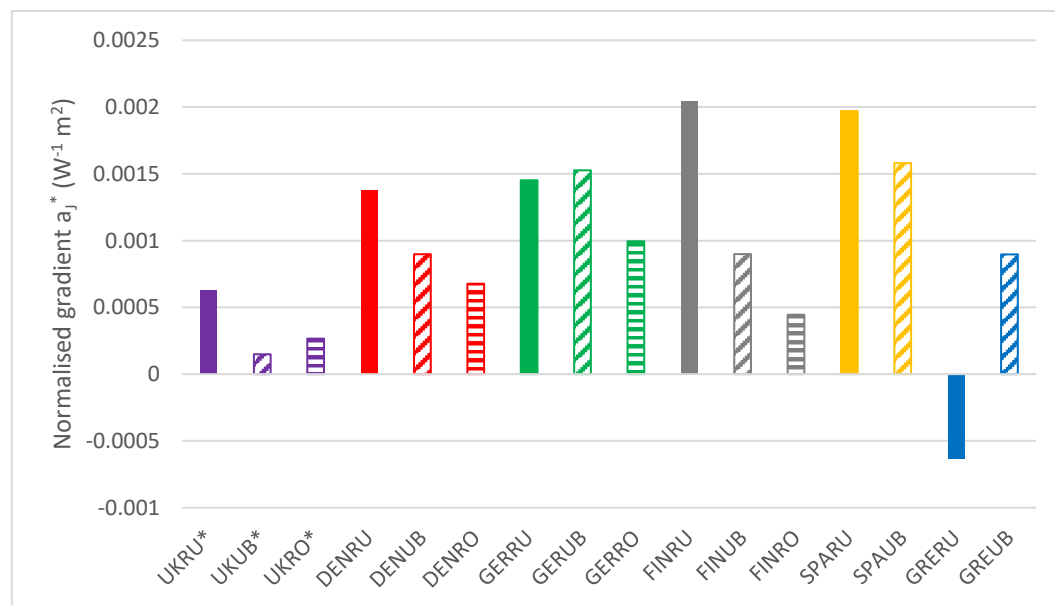


**Figure 3:** Normalised slopes  $a_j^*$  for  $K_{\downarrow}$  (\*UK sites are calculated with solar irradiance).

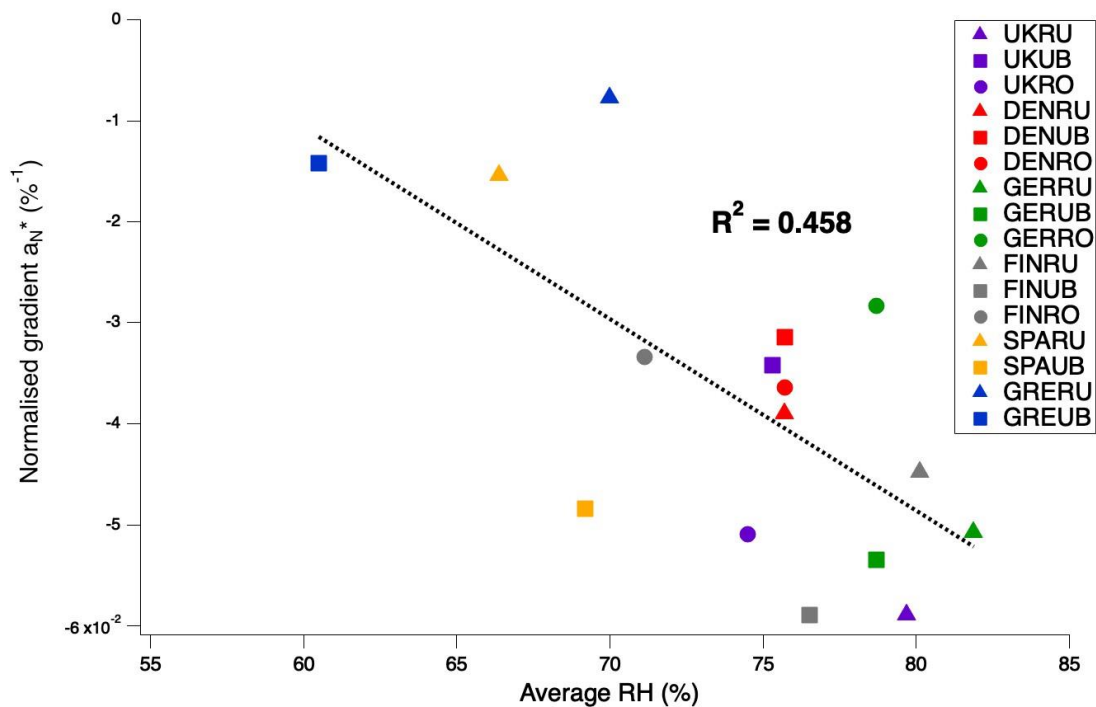


**Figure 4:** Relationship of average relative humidity and normalised gradients  $a_N^*$ .

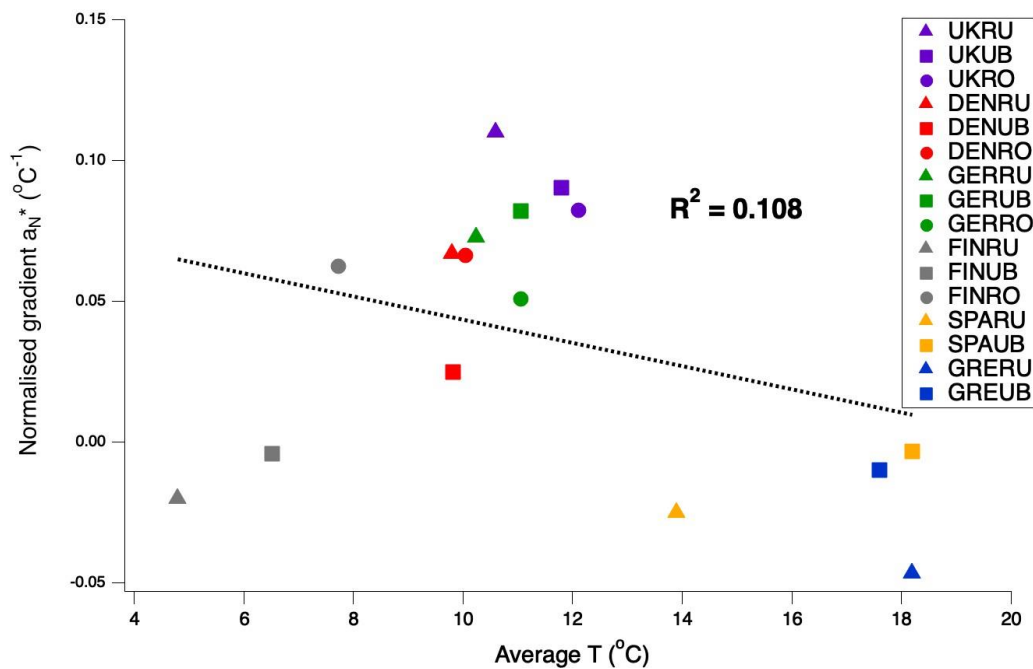
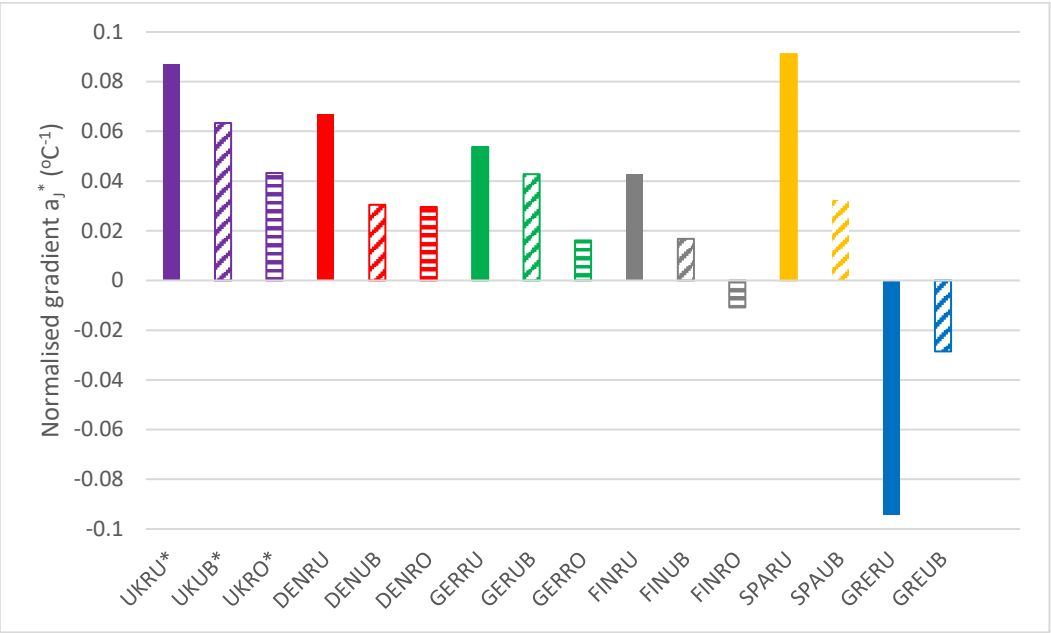


**Figure 5:** Relationship of average temperature and normalised gradients  $a_N^*$ .



1660 **Figure 6:** Normalised gradients  $a_j^*$  for temperature.

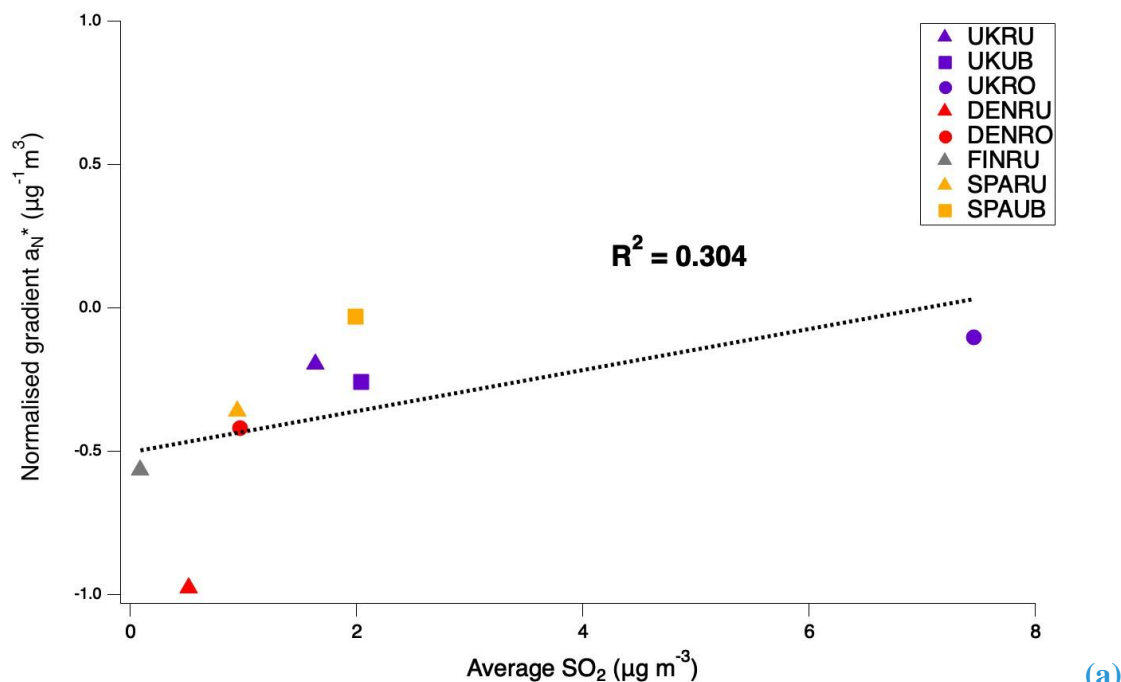


**Figure 7a:** Relationship of average  $\text{SO}_2$  concentrations and normalised gradients  $a_N^*$  for the sites with available data (a) and for the sites with available data excluding UKRO (b).

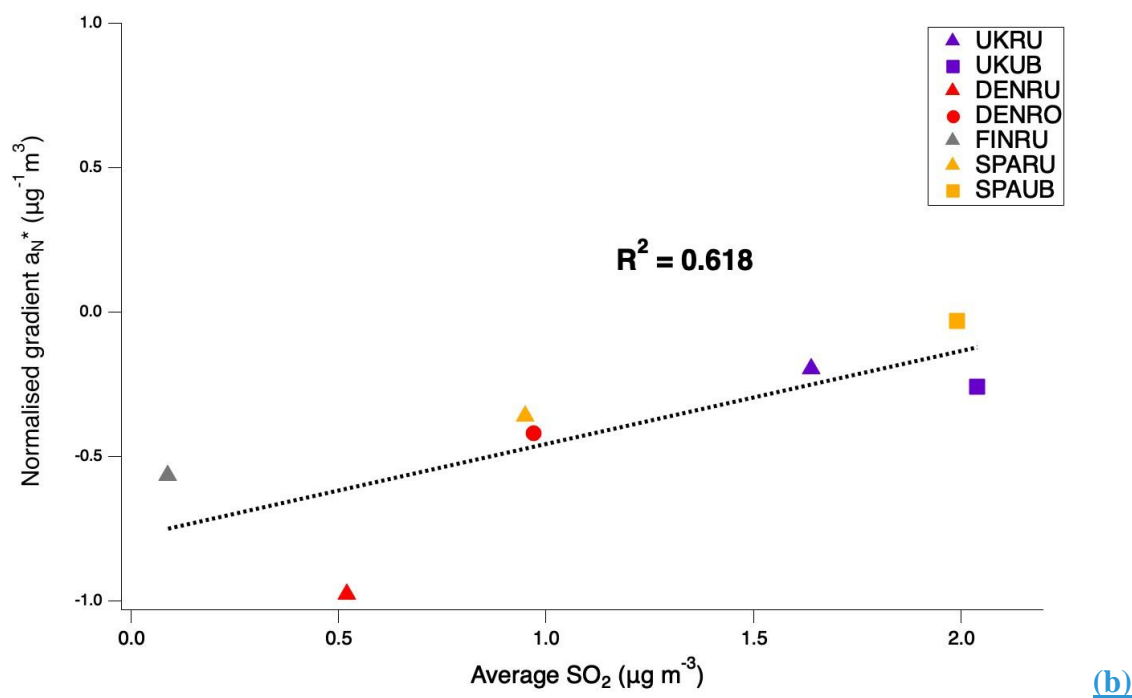


**Figure 7b:** Relationship of average  $\text{SO}_2$  concentrations and normalised gradients  $a_N^*$  for the sites with available data (a) and for the sites with available data excluding UKRO (b).

Relationship of average SO<sub>2</sub> concentrations and normalised gradients  $a_N^*$  (UKRO not included).

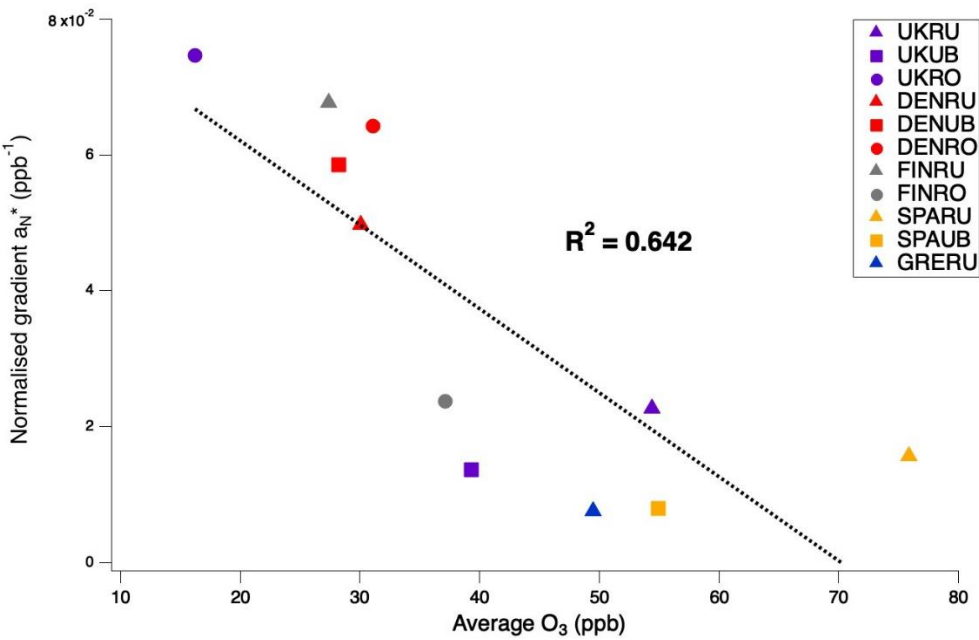


Figure 8: Relationship of average O<sub>3</sub> concentrations and normalised gradients  $a_N^*$ .